BRITISH GEOLOGICAL SURVEY
MARINE OPERATIONS RESEARCH PROGRAMME

MARINE REPORT 87/38

WB/MR
87/38

GEOPHYSICAL INTERPRETATIONS

IN THE CELTIC SEA

AND

SOUTH WESTERN APPROACHES

by

M BRIANT

Murchison House
West Mains Road
Edinburgh EH9 3LA

Tel: 031-667 1000
Telex: 727343
Fax: 031-668-2683

October 1987

CONTENTS

PREFACE

During my year as a Sandwich Course student at British Geological Survey, from August 1986 to August 1987, I have been involved in a number of projects in the Celtic Sea and South-Western Approaches area. This report describes some of these projects.

FIGURES

TABLES

CHAPTER 1

RELEASED WELLS IN THE SOUTH-WESTERN APPROACHES AND WESTERN ENGLISH CHANNEL

1.1 Introduction

Seven wells have been drilled and released in the South-Western Approaches and western English Channel area. Four were drilled by the Institute of Geological Sciences for the Department of Energy in 1977 using a semi-submersible drilling vessel, Zephyr (88/2-1, 87/14-1, 87/18-1 and 83/24-1). (Evans et al 1981).

86/18-1 and 72/10-1A were drilled by the Atlantic Drilling Company for the British National Oil Corporation in 1979 using a drilling vessel Atlantic 1.

87/12-1A was drilled by BP Petroleum Development Limited in 1979.

Fig 1.1 shows the positions of these wells and the known solid geology of the area (after Evans 1985 a, b; Evans 1982; Evans et al 1984; Holder et al 1983 and Taylor et al 1980).

This report consists of:

a) Brief details on each well
b) Tables showing the depths of noticible, sudden changes in sonic log velocities in each well.
c) Tables showing sonic log velocities, depth and lithology throughout each well.
d) A graphic log for each well.

1.2 Brief Details Of Wells

88/2-1 (Tables 1.1 and 1.8, Fig 1.2)

This well was drilled to provide information on the pre-late Cretaceous Strata of the block 88/2 area, and to investigate a suggested thick fault-bounded wedge of Jurassic sediments, underlain by Permo-Triassic strata. Cretaceous Chalk is known to occur at the sea bed in the vicinity. (Taylor et al 1980).

87/14-1 (Tables 1.2 and 1.9, Fig 1.3)

This well was drilled to investigate the strata present beneath a southward-dipping Tertiary and late Cretaceous sequence. Shallow drilling and sea bed sample data proved a thin early Cretaceous sequence overlying early Jurassic sediments in the area to the north of the site (Wilkinson and Halliwell, 1980). The well was drilled to find the extent of the early Jurassic sequence. Palaeogene sediments are at the sea bed in this area (Holder et al 1983).

87/16-1 (Tables 1.3 and 1.10, Fig 1.4)

This well was drilled to provide information on pre-late Cretaceous strata in the central part of block 87, slightly north of the Tertiary basinal axis in an area where, from seismic evidence, a thin Jurassic or Early Cretaceous succession was believed to occur between the Chalk and Permo-Triassic rocks. Paleogene sediments are known to be at the sea bed in this area (Holder et al 1983).

83/24-1 (Tables 1.4 and 1.11, Fig 1.5)

This well was drilled on the southern side of the Scilly-Cornubian High, a south-westerly extension of the basement high which separates Mezozoic basins in the South-Western Approaches from those in the Celtic Sea. Reflection seismic data indicated a thin northwards dipping wedge of sediments overlying the basement at the borehole site. The borehole was drilled to penetrate this wedge which was thought to consist of pre-Cretaceous Mesozoic rocks beneath Chalk.

86/18-1 (Tables 1.5 and 1.12, Fig 1.6)

This well was drilled on a basement high at the northern edge of the South-Western Approaches basin. Paleogene sediments are known to be at the sea bed in this area. (Holder et al 1983).

72/10-1A (Tables 1.6 and 1.13, Fig 1.7)

Initial drilling of this well (72/10-1) was abandoned due to a 20" casing failure, drilling was resumed at a new position close to the original borehole (72/10-1A). The well was drilled close to the edge of the continental shelf within the South-Western Approaches basin. Quaternary sediments were found in this area. (Evans 1985).

87/12-1A (Tables 1.7 and 1.14, Fig 1.8)

This well was drilled on a basement high to the north of the South Western Approaches Basin. Upper Cretaceous Chalk is known to be at the sea bed in this area. (Holder et al 1983).

1.3 Conclusions

All seven wells show a thick layer of Cretaceous Chalk with a thickness of between 375 and 549m where tertiary material is present. Where the Tertiary material is absent chalk outcrops at the seabed (87/12-1A and 88/2-1). The sonic velocities within the Chalk cover a range between 2.44 and 4.35 kms^{-1}, but a sonic velocity of as high as 5.08 kms^{-1} was reached in 87/12-1A.

Lower Cretaceous deposits are either thin or absent in the wells and consist mainly of mudstone, siltstone, sandstone and claystone. The thickness sequence, found in 87/12-1A, is 123m thick and deposits are absent in wells 88/2-1 and 87/14-1.

Only two wells show any Jurrasic strata; 88/2-1 shows a thick sequence (491m) of mudstone, shale and limestone interbeds; 72/10-1A shows interbeds of volcanic material and claystone through both lower Cretaceous and Jurassic strata.

Sonic velocities within the lower Cretaceous and Jurassic strata vary between 2.03 and 3.39 kms^{-1}, and sonic velocities of up to 5.08 kms^{-1} were recorded for the volcanic material in 72/10-1A.

All seven wells penetrated Permo-Triassic material although four of them do not cover the whole sequence (87/14-1, 87/16-1, 88/2-1, 72/10-1A). The thickness of the strata varies considerably from 51m in 83/24-1 to over 2 km in 72/10-1A. Sonic velocities within the strata cover a wide range, dependent on lithology and depth, mainly between 2.54 and 4.35 kms^{-1}, but sonic velocities of up to 6.10 kms^{-1} were recorded in 72/10-1A where the depth of Permo-Triassic material is greater than 3700m, and velocities between 4.35 and 5.08 kms^{-1} were recorded in wells 88/2-1 and 86/18-1. Well 72/10-1A shows Devonian limestone with sonic velocities between 4.9 and 6.10 kms^{-1}. See Table 1.15 for a summary of sonic velocities.

TABLE 1.1 - **Major Changes in Sonic Velocity in Well 88/2-1)**

Depth (m)	Comments	Drop/Rise	From (kms^{-1})	To (kms^{-1})
214.5	Bottom of Cretaceous Chalk	Drop	3.39	2.18
340-370	First limestone in Jurassic	Rise	2.18	2.44
665.0	Layer of limestone	Rise	3.39	4.69
725.5	Below top of Permo-Triassic Siltstone/Mudstone	Drop	4.35	3.21

TABLE 1.2 - **Major Changes in Sonic Velocity in Well 87/14-1**

Depth (m)	Comments	Drop/Rise	From (kms^{-1})	To (kms^{-1})
540.0	Cretaceous Chalk grading to limestone	Rise	3.21	3.81
692.5	Top of Permo-Triassic. Sandstone Mudstone and Siltstone	Drop	4.06	3.39
845.0	Intra Permo-Triassic, Sandstone, Mudstone and Siltstone	Rise	3.39	3.81

TABLE 1.3 - **Major Changes in Sonic Velocity in Well 87/16-1**

Depth (m)	Comments	Drop/Rise	From (kms^{-1})	To kms^{-1})
533.00	Cretaceous Chalk (Turonian)	Rise	3.21	3.81
791.8	Early Cretaceious Mudstone/ Sandstone	Drop	4.69	3.05
829.5	Triassic Mudstone	Rise	3.05	3.39

TABLE 1.4 - **Major Changes in Sonic Velocity in Well 83/24-1**

Depth (m)	Comments	Rise/Drop	From (kms^{-1})	To (kms^{-1})
720	Cretaceous Chalk (Cenomonian)	Rise	3.05	3.59
780	Cretaceous Chalk becoming increasingly glauconitic	Rise	3.39	4.35
830	Lower Cretaceous Sandstone	Drop	4.69	2.34
853	Permo-Triassic Mudstone	Rise	2.44	3.05
922	Carboniferous-Devonian Slate	Rise	3.81	4.69

TABLE 1.5 - **Major Changes in Sonic Velocity in Well 86/18-1**

Depth (m)	Comments	Drop/Rise	From (kms^{-1})	(To (kms^{-1})
832.1	Cretaceous Chalk (Coniacian-Turonian)	Rise	3.81	4.35
883.9	Cretaceous Chalk/Sandstone boundary	Drop	4.35	2.65
887.0	Cretaceous Calcareous Sandstone	Rise	2.65	5.08
900.7	Lower Cretaceous Sandstone	Drop	4.69	2.77
1008.9	Lower Cretaceous. Wealden Siltstone, Claystone and Sandstone - Triassic Interbedded Siltstone Claystone and Sandstone	Rise	2.77	3.05
1822.7	Early upper Permian or Late Lower Permian Claystone with Dolomite traces	Rise	4.35	5.08
2433.8	Late Devonian-Carboniferous Shale	Rise	4.69	5.54

TABLE 1.6 - **Major Changes in Sonic Velocity in Wells 72/10-1, 72/10-1A**

Depth (m)	Comments	Drop/Rise	From (kms^{-1})	To (kms^{-1})
676.7-701.0	Late Eocene Limestone	Rise	2.77	3.05
731.5	Middle Eocene Limestone (Traces of Chert)	Drop	3.05	2.90
762.0	Middle Eocene Limestone	Rise	2.90	3.21
780.3	Middle Eocene Limestone and Claystone	Drop	3.21	2.26
816.9	Middle Eocene Sandstone	Rise	2.44	3.21
940.3	Early Eocene Claystone	Drop	3.05	2.34
1019.9	Upper Cretaceous Chalk	Rise	2.54	2.90
1408.8	Early Cretaceous Claystone	Drop	3.81	2.65
1417.3	Early Cretaceous Volcanics	Rise	2.65	3.39
1420.4	Early Cretaceous Claystone	Drop	3.39	2.65
1428.0	Early Cretaceous Volcanics	Rise	2.65	4.69
1438.7	Early Cretaceous/ Jurassic Claystone	Drop	4.69	3.05
1468.5	Permo-Triassic Limestone/Claystone	Rise	3.05	4.06
1484.4	Permo-Triassic Claystone	Drop	4.06	3.05
1490.5	Permo-Triassic Limestone	Rise	3.05	5.54
1505.7	Permo-Triassic Claystone	Drop	5.54	2.77
1964.4	Permo-Triassic Halite	Rise	4.06	4.69
2660.9	Permo-Triassic Claystone	Rise	4.35	5.08
2877.3	Permo-Triassic Sandstone	Drop	5.08	4.69

TABLE 1.7 - **Major Changes In Sonic Velocity In Well 87/12-1A**

Depth (m)	Comments	Drop/Rise	From (kms^{-1})	To (kms^{-1})
342	Early Cretaceous, Limestone/Greensand boundary	Drop	3.81	2.54
465	Top of Triassic Mudstone occasionaly grading to Siltstone with Anhydrite	Rise	2.54	3.21
757	Triassic Mudstone	Rise	3.59	4.69
780	Triassic Mudstone	Drop	4.69	3.21
1745-1780	Top of Devonian Limestone	Rise	4.35	6.10
2100	Devonian Mudstone with Sandstone	Drop	6.10	5.08

TABLE 1.8 - **Sonic Velocities through Well 88/2-1**

Position: 49° 51' 13.9"N
03° 47' 21.2"W

Depth (m) Below K.B.	Velocities (Kms^{-1})	Comments	Lithology
25	-	Sea level	
100	-	Sea-bed	Cretaceous Chalk (Solid Geol.)
165	-	First Returns	
165-214.5	2.90-3.39	Velocity increases with depth from 2.90Kms^{-1} at 165m to 3.39Kms^{-1} at 214.5m	
214.5-222	2.26-2.34	Velocity - variable	Jurassic Mudstone
222-235	2.44-2.77	On average velocity increases from 2.54Kms^{-1} to 2.65 km S^{-1}	Jurassic - Traces of Pebbles in Mudstone
235-320	2.18-2.54	Velocity variable	Jurassic Mudstone
320-340	2.03-2.26	Lowest velocity ~2.03Kms^{-1} at 335m	Jurassic Mudstone-Silty
340-360	2.26-2.90	Velocity - Considerable variation	Jurassic Mudstone-Bands of Shale
360-370	2.18-2.26		Jurassic Mudstone
370-670	2.18-2.65 2.65-3.39	Highest velocity ~4.69Kms^{-1}	Jurassic Mudstones Interbedded Sandstone
670-695	4.35-6.10		Jurassic Mudstone with high Limestone concentration
702-725.5	4.35-4.69		Triassic/Rhaetic Mainly Limestone
725.5-766.5	2.65-3.81		Triassic/Rhaetic Mudstone interbedded with Limestone and Siltstone
766.5-870	3.05-3.39		Triassic Mudstone, Limestone and Dolomite

TABLE 1.9 - **Sonic Velocities through Well 87/14-1**

Position: 49° 32' 02.3"N
04° 12' 25.6"W

Depth (m) Below K.B.	Velocities (Kms^{-1})	Comments	Lithology
25	-	Sea level	
110	-	Sea-bed	Palaeogene. Eocene Limestones and Sandstones
162	-	First Returns (Bulk Density)	
162-202.5	-		Palaeogene. Eocene Limestones and Sandstones, Palaeocene Clay
202.5-250	-		Palaeogene. Danian Chalk
250-354	-		Cretaceous Chalk
354	-	First Returns (Sonic log)	
354-540	2.65-3.39	Velocity increases with depth from $2.65Kms^{-1}$ at 354m to $3.39Kms^{-1}$ at 475m	Cretaceous Chalk Campanian - Coniacian
540-692.5	3.59-4.35	Velocity increases with depth from $3.59Kms^{-1}$ at 550m to 4.35 at 650m	Cretaceous Chalk Turonian - Cenomanian
692.5-710	3.05-3.39		Permo-Triassic Sandstone/ Mudstone
710-730	3.21-3.81		Permo-Triassic Sandstone/ Mudstone/Siltstone
730-845	3.05-3.39		Permo-Triassic. Interbedded Sandstone, Mudstone, Siltstone
845-1232.8	3.39-4.35	Velocity - Variable	Permo-Triassic. Interbedded Sandstone, Mudstone and Siltstone

TABLE 1.10 - **Sonic Velocities Through Well 87/16-1**

Position: 49° 26' 21.671"N
04° 53' 17.370"W

Depth (m) Below K.B.	Velocities (kms^{-1})	Comments	Lithology
25.5	-	Sea level	
121.3	-	Sea-bed	Palaeogene. Limestones and Sandstones
177	-	First Returns	
177-242	2.18-2.65	Velocity -Variable	Palaeogene. Eocene Limestone
242-295.7	2.54-2.77		Cretaceous Chalk
295.7-533	2.77-3.21	Velocity increases from $2.77kms^{-1}$ at 295.7m to $3.21kms^{-1}$ at 465m	Cretaceous Chalk
533-791.75	3.39-4.69	Velocity increases from $3.39kms^{-1}$ at 545m to $4.69kms^{-1}$ at 791m	Cretaceous Chalk
791.75-829.5	2.54-3.05	Velocity - Variable	Cretaceous Mudstone and Sandstone
829.5-929.5	2.90-3.59		Triassic Mudstone

TABLE 1.11 - **Sonic Velocities Through Well 83/24-1**

Position: 49° 10' 35.1"N
08° 20' 34.3"W

Depth (m) Below K.B.	Velocities (kms^{-1})	Comments	Lithology
25.5	-	Sea level	
161.5	-	Sea-bed	Neogene Clay and Sandstone
213.0	-	First Returns (Bulk Density)	
213-249	-	No Sonic log	Neogene Clay and Sandstone
249-431	-	No Sonic log	Palaeogene Sandstone Limestone and Clay
431-460	-	No Sonic Log	Cretaceous Chalk
460	-	First Returns (Sonic Log)	
460-720	3.05-3.59	Velocity increases with depth from $2.44kms^{-1}$ at 500m to $3.21kms^{-1}$ at 665m	Cretaceous Chalk
720-780	3.05-3.59		Cretaceous Chalk Dolomite traces
780-806	4.06.4.69	Velocity reaches maximum of $5.08kms^{-1}$ at 795m	Cretaceous Chalk traces of Flint. Increasingly glauconitic
806-830	2.54-4.35	Velocity - many peaks between $2.54kms^{-1}$ and $4.35kms^{-1}$	Lower Cretaceous Limestone and Clay Interbedded
830-853	2.18-2.44		Lower Cretaceous Clay grading to Mudstone with interbedded Sandstone
853-922	2.90-4.06	Velocity increases with depth from $2.90kms^{-1}$ at 853m to $4.06kms^{-1}$ at 910m.	Permo-Triassic Mudstone, Siltstone and Sandstone
922-1044	4.06-5.08	Velocity increases with depth from $4.06kms^{-1}$ at 990m to $5.08kms^{-1}$ at 1036m	Carboniferous-Devonian Slate with interbedded Sandstone and Mudstone

TABLE 1.12 - **Sonic Velocities Through Well 86/18-1**

Position: 49° 21' 28.67"N
05° 33' 54.85"W

Depth (m) Below K.B.	Velocities (kms^{-1})	Comments	Lithology
25	-	Sea level	Palaeogene (Solid Geology)
266.7	-		Palaeocene Claystones
397.2	-		Cretaceous Chalk
536.1	-	First returns	
536.1-829.1	2.77-3.81	Velocity increases with depth from $2.77kms^{-1}$ at 536m to $3.81kms^{-1}$ at 747m	Cretaceous Chalk
829.1-883.9	3.81-4.35	Velocity reaches a maximum of $5.08kms^{-1}$ at 814m	Cretaceous Limestone
883.9-900.7	3.81-5.08	Low velocity for 2m at Limestone/Sandstone boundary $2.65kms^{-1}$	Cretaceous Sandstone
900.7-1011	2.54-3.05		Lower Cretaceous Sandstone
1011-1033.6	2.34-2.77	Velocity - variable	Lower Cretaceous Wealden Sandstone
1033.6-1082.0	2.54-3.39	Velocity - considerable variation	Triassic. Inter-bedded Siltstone, Claystone and Sandstone
1802.0-1444.8	3.21-3.81	Velocity increases with depth from $3.21kms^{-1}$ at 1082.0m to $3.81kms^{-1}$ at 1201m, shows considerable variation	Triassic/Permo-Triassic. Inter-bedded Siltstone, Claystone and Sandstone grading to Siltstone
1444.8-1822.7	3.81-4.35		Permo-Triassic Siltstone
1822.7-2432.3	4.35-5.08		Permian interbedded Shales grading to Sandstones

TABLE 1.12 (Cont.)

Depth (m) Below K.B.	Velocities (kms^{-1})	Comments	Lithology
2432.3-2517.6	$\sim$ 5.08	Very few variations in velocity	Late Devonian-Carboniferous Shale

TABLE 1.13 - **Sonic Velocities Through Wells 72/10-1, 72/10-1A**

Positions: 1) 48° 47' 22.85"N 1A) 48° 47' 23.4"N
09° 06' 01.76"W 09° 06' 01.9"W

Depth (m) Below K.B.	Velocities (kms^{-1})	Comments	Lithology
25.6	-	Sea level	
182.6	-	Seabed	Neogene Clay (Solid Geol.)
288.6	-	First Returns	
288.6-365.8	1.91-2.18		Neogene Clay
365.8-676.7	2.18-2.54	Velocity increases with depth from 2.18kms^{-1} at 442.0m to 2.54kms^{-1} at 676.7m	Neogene Clay/Sand/ Sandstone, Palaeogene Clay/Sand/Sandstone Limestone.
676.7-777.2	2.54-3.39		Palaeogene Limestone
777.2-816.9	-	Bottom of 72/10-1	Palaeogene Limestone/ Clay
816.9-940.3	3.05-3.39		Palaeogene Sandstone/ Claystone
940.3-1019.9	2.03-2.77	Velocity - highly erratic	Palaeogene Claystone/ Siltstone
1019.9-1408.8	2.77-4.35	Velocity increases with depth from 2.77kms^{-1} at 1019.9m to 4.35kms^{-1} at 1408.8m	Cretaceous Chalk/Limestone
1408.8-1417.3	2.54-2.77		Cretaceous Claystone/ Volcanics
1417.3-1420.4	3.21-3.81		Cretaceous Volcanics
1402.4-1429.5	2.34-2.54		Cretaceous Claystone/ Volcanics
1429.5-1438.7	4.35-5.08		Cretaceous Volcanics
1438.7-1444.8	2.34-3.05	Velocity drops with depth from 3.05kms^{-1} at 1438.7m to 2.34kms^{-1} at 1444.8m	Cretaceous Claystone/ Volcanics
1444.8-1465.5	2.77-2.90	A velocity Peak between 1444.8 and 1447.8m of 3.05kms^{-1}	Jurassic Claystone
1465.5-1469.1	2.77-3.39	Velocity - highly variable	Permo-Triassic Claystone

TABLE 1.13 Cont.)

Depth (m) Below K.B.	Velocities (kms^{-1})	Comments	Lithology
1469.1-1479.5	4.06-4.35		Permo-Triassic Limestone/Claystone
1479.5-1490.5	3.05-4.35	Velocity drops from $4.35kms^{-1}$ at 1479.5m to $3.05kms^{-1}$ at 1486m and then rises to $6.10kms^{-1}$ at 1490.5m	Permo-Triassic. Interbedded Limestone and Claystone
1490.5-1502.7	5.08-6,10	Velocity drops with depth from $5.54kms^{-1}$ at 1496.6m to $3.05kms^{-1}$ at 1502.7m	Permo-Triassic Limestone
1502.7-1950.7	2.77-4.06	Velocity increases with depth from $2.77kms^{-1}$ at 1508.8m to $4.06kms^{-1}$ at 1859.3m	Permo-Triassic Claystone with Anhydrite interbeds and bands of Siltstone
1950.7-1966.0	4.06-4.35	Velocity increases with depth from $4.06kms^{-1}$ at 1950.7m to $4.35kms^{-1}$ at 1966.0m	Permo-Triassic Siltstone
1966.0-2453.6	$\sim$ 4.35	Velocity drops to $3.59kms^{-1}$ at short bands of Claystone and $3.81kms^{-1}$ for Siltstone	Permo-Triassic Halite with bands of Claystone and Siltstone
2453.6-2499.4	3.81-5.08	Velocity - erractic	Permo-Triassic interbeds of Claystone, and Sandstone with traces of Halite
2499.4-2660.9	$\sim$ 4.35		Permo-Triassic Halite
2660.9-2743.2	4.35-5.08		Permo-Triassic interbeds of Claystone and Siltstone
2743.2-2865.1	4.35-5.54		Permo-Triassic Claystone
2865.1-3218.7	4.35-5.08		Permo-Triassic Sandstone band of Siltstone between 3106m and 3127m

TABLE 1.13 - (Cont.)

Depth (m) Below K.B.	Velocities (kms^{-1})	Comments	Lithology
3218.7-3371.1	4.35-5.08		Permo-Triassic. Interbedded Breccio-Conglomerate and Sandstone
337.1-3.702.1	4.69-5.08	Velocity varies very little	Permo-Triassic Breccio-Conglomerate

TABLE 1.14 Sonic velocities through well 87/12-1A

Position; 49° 34' 19.985" N
04° 43' 25.995" W

Depth (m) Below K.B.	Velocities (kms^{-1})	Comments	Lithology
25.9	-	Sea level	
116.8	-	Sea bed	Cretaceous Chalk (Solid Geol.)
200 200-342	- 3.39-5.08	First returns Velocity increases with depth from 3.59kms^{-1} at 200m to 4.35kms^{-1} at 340m	Cretaceous Limestone/ undifferentiated Chalk
342-415	2.18-3.05		Cretaceous Sandstone/ Mudstone
415-422.5	2.34-2.77		Early Cretaceous, Wealden Mudstone/ Sandstone
422.5-450	2.10-3.21	Velocity-Variable	Early Cretaceous Sandstone/Mudstone
450-465	2.10-3.21	Velocity-Occasionally outside region	Early Cretaceous Mudstone/Sandstone
465-760	3.05-3.81	Velocity-variable between 570m and 650m gradual increase from 3.05kms^{-1} at 465m to 3.81kms^{-1} at 760m	Late Permo-Triassic Mudstone with Anhydrite (465-700m) Sandstone (520-545m) and (695-760m), Siltstone (560-760m)
760-790	3.05-5.54	Velocity drops from 5.54kms^{-1} at 760m to 3.39kms^{-1} at 780m	Late Permo-Triassic Sandstone grading to Mudstone
790-1746	3.05-5.08	Gradual rise in velocity with depth from 3.05kms^{-1} at 790m to 5.08kms^{-1} at 1575m	Permo-Triassic Inter-bedded Mudstone, Sandstone and Siltstone
1746-1763	5.08-6.10		Permo-Triassic Undifferentiated Conglomerate

TABLE 1.14 cont.

Depth (m) Below K.B.	Velocities (kms^{-1})	Comments	Lithology
1763-1775	~5.08		Middle Devonian Sandstone
1775-1779	4.06-4.35	Low Velocity at 1779m of $3.81 kms^{-1}$	Middle Devonian Mudstone
1779-2045	~6.10	A few Velocity lows of ~$5.54 kms^{-1}$ Associated with Sandstone	Devonian Limestone
2045-2102.5	5.08-6.10		Devonian Limestone/ Mudstone
2102.5-2225	4.35-5.54		Devonian Interbedded Mudstone and Sandstone
2225-2242	~4.90		Devonian Sandstone

TABLE 1.15 Summary of sonic velocities through the wells

PERIOD	LITHOLOGY	VELOCITY(kms^{-1})	WELL
NEOGENE	Clay	1.91-2.18	6
PALAEOGENE	Limestone	2.18-2.65	1,6
	Sandstone/Claystone/Siltstone	2.18-3.39	1,4,6
UPPER CRETACEOUS	Chalk	2.43-4.69	ALL
	Chalk	4.69-5.08	7
LOWER CRETACEOUS	Mudstone/Sandstone/Claystone	2.10-3.21	3,4,5,6,7
	Limestone/Claystone	2.54-4.35	4
	Volcanics/Claystone	3.21-3.81	6
	Volcanics	4.45-5.08	6
JURASSIC	Mudstone/Shale	2.03-2.90	1
	Claystone	2.77-2.90	6
	Limestone	4.35-6.10	1
PERMO-TRIASSIC	Claystone/Siltstone/Sandstone	2.55-3.96	4,6
	Mudstone/Sandstone/Claystone/ Siltstone/Limestone	2.90-4.35	1,2,3, 4,6,7
	Limestone/Claystone	3.05-4.35	6
	Claystone/Sandstone/Halite	3.81-4.98	6
	Halite	4.35	6
	Limestone	4.35-4.69	1
	Limestone	5.08-6.10	6
	Shale/Sandstone	4.35-5.08	4
	Sandstone/Siltstone	4.35-5.08	6
	Claystone	4.35-5.54	6
	Breccio-Conglomerate	4.35-6.10	6,7

TABLE 1.15 cont.

PERIOD	LITHOLOGY	VELOCITY(kms^{-1})	WELL
CARBONIFEROUS-DEVONIAN	Mudstone/Slate/Sandstone	4.35-5.54	4,7
	Shale	5.08	4
	Mudstone/Limestone	5.08-6.10	7
	Limestone	6.10	7

1 = 88/2-1 3 = 87/16-1 5 = 86/18-1 7 = 87/12-1A
2 = 87/14-1 4 = 83/24-1 6 = 72/10-1A

Fig 1.1 Solid geology and positions of released wells in the South Western Approaches and western English Channel.(After Evans.1985,Evans.1982,Evans et al.1984,Holder et al.1983 and Taylor et al.1980).

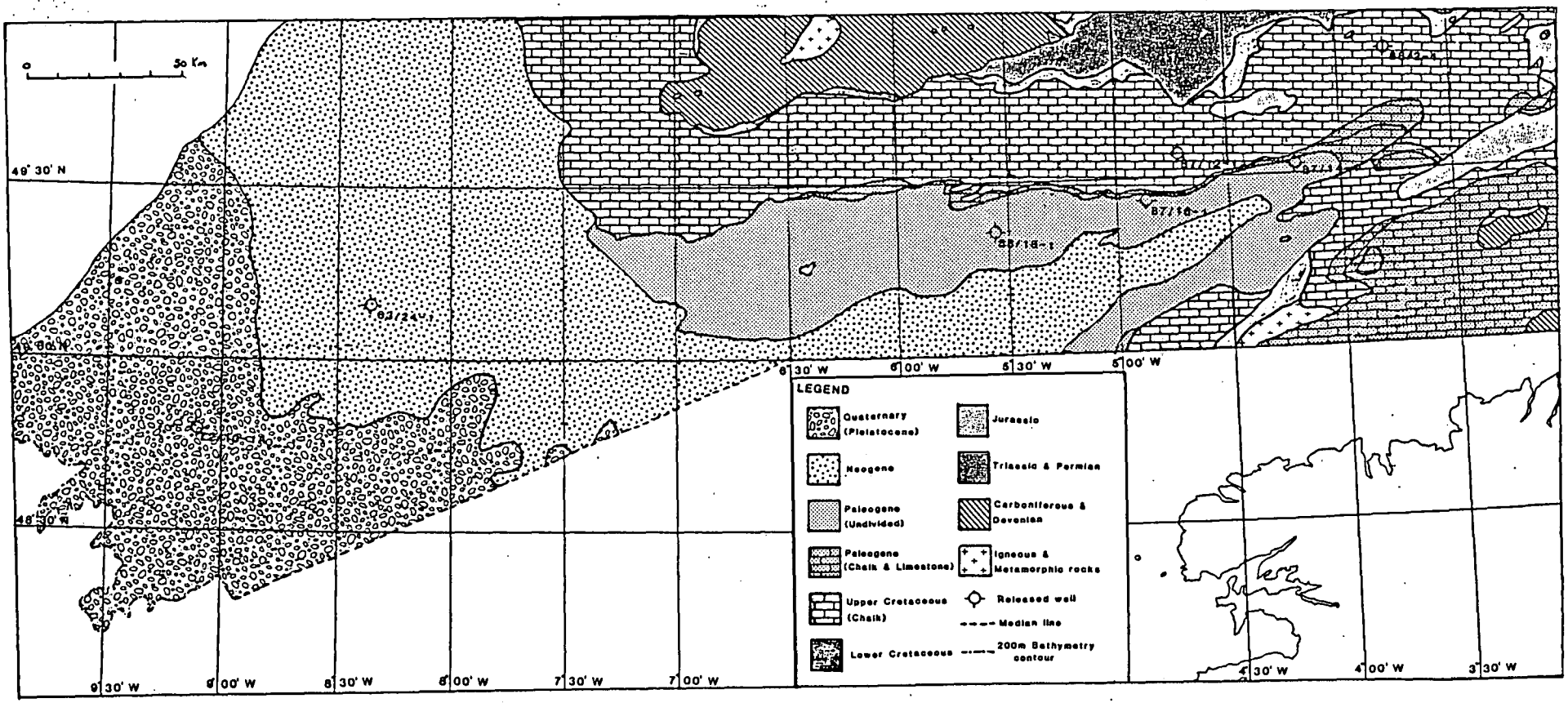

Fig 1.2 Summary of succession in well 88/2-1 (After Evans et al.1981)

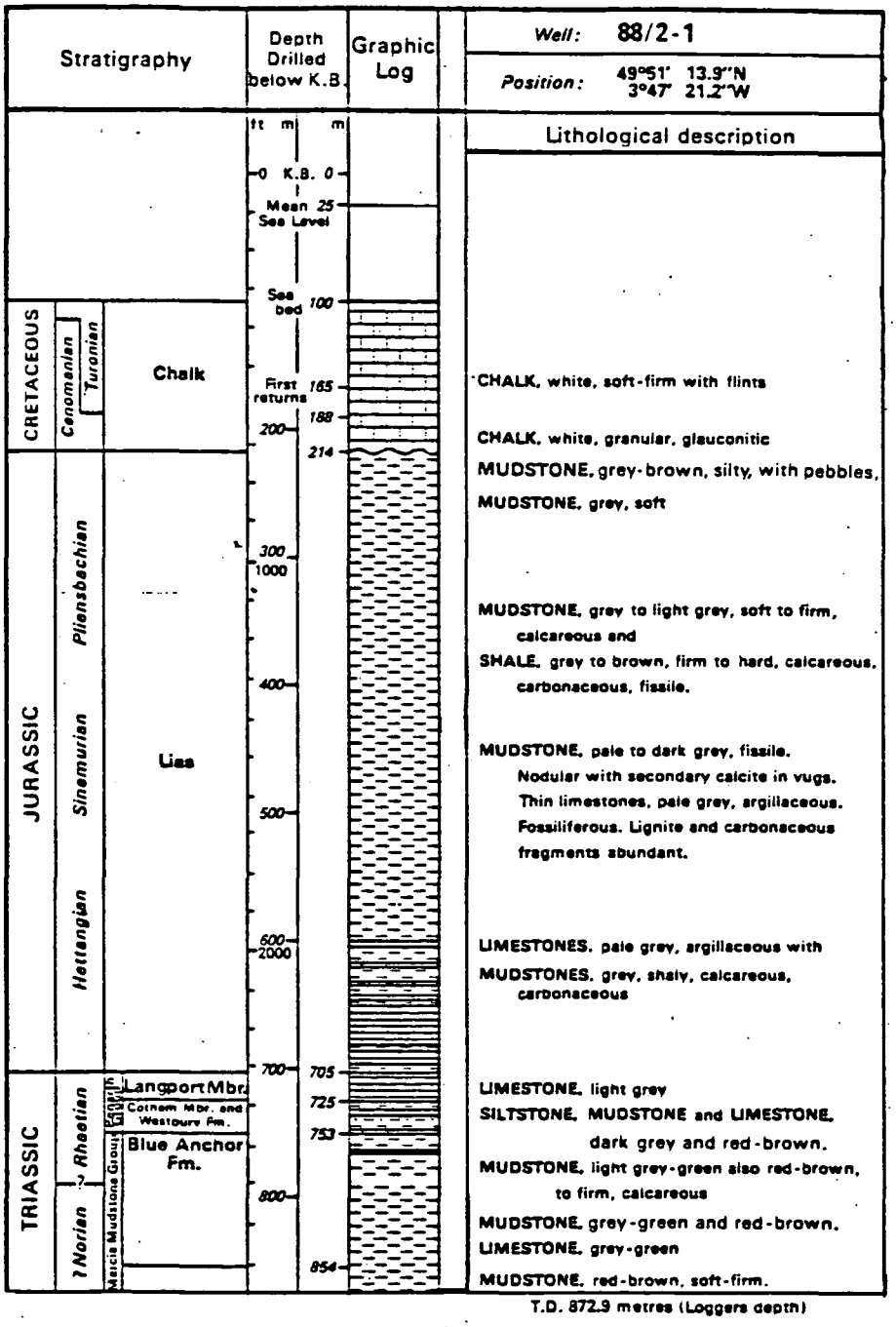

T.D. 872.9 metres (Loggers depth)

Fig 1.3 Summary of succession in well 87/14-1 (After Evans et al.1981)

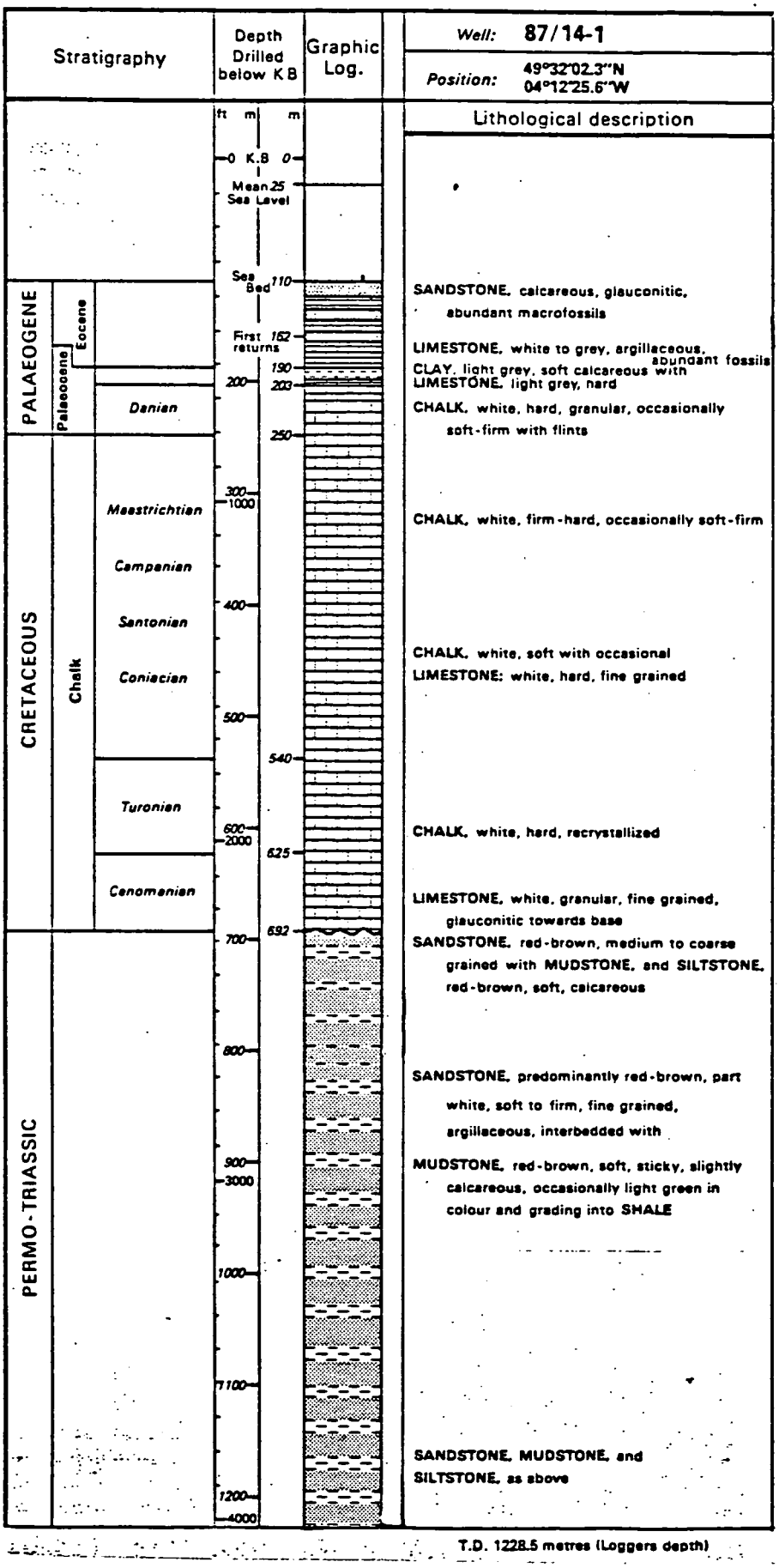

Fig 1.4 Summary of succession in well 87/16–1 (After Evans et al.1981)

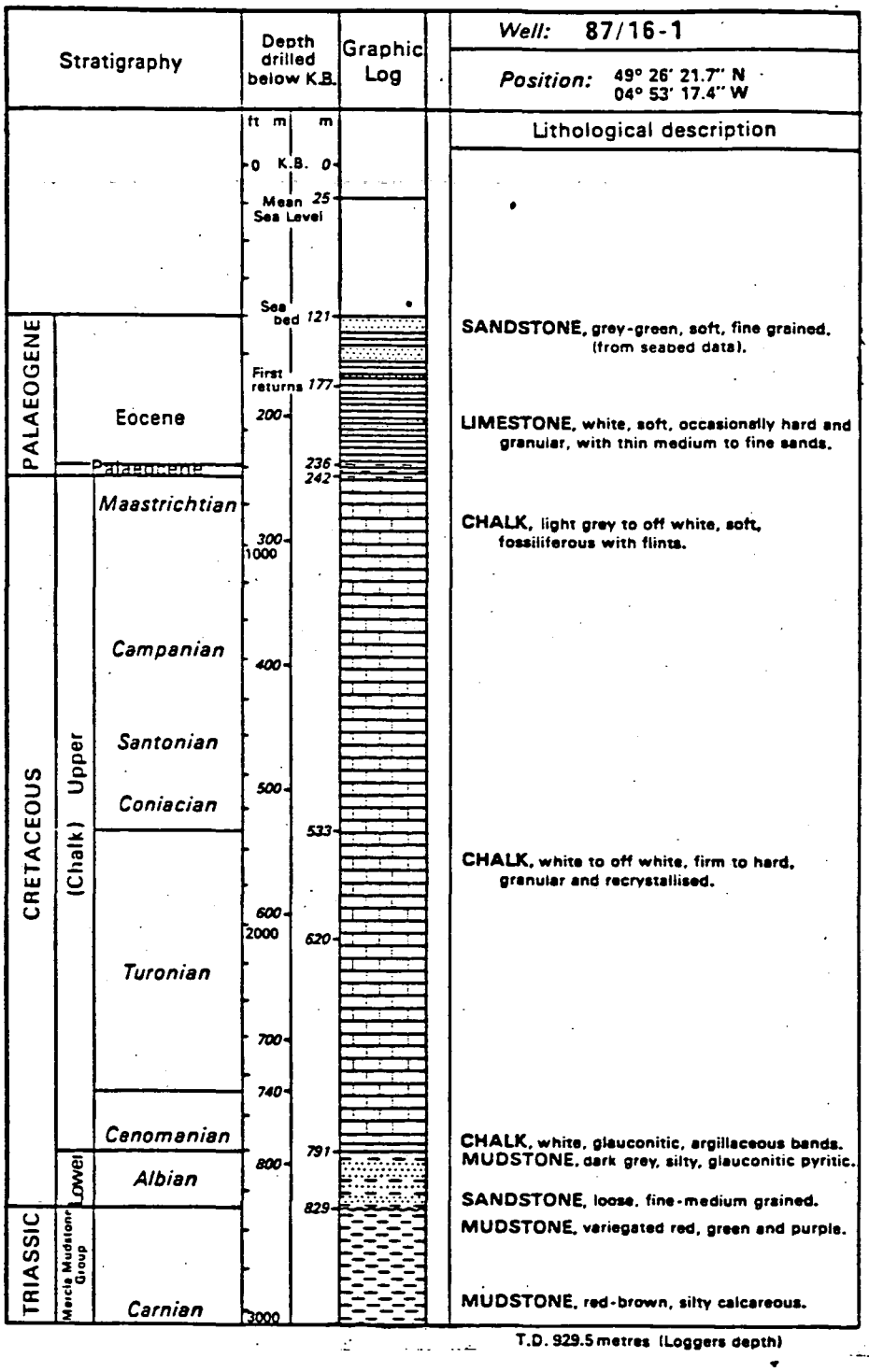

Fig 1.5 Summary of succession in well 83/24-1 (After Evans et al.1981)

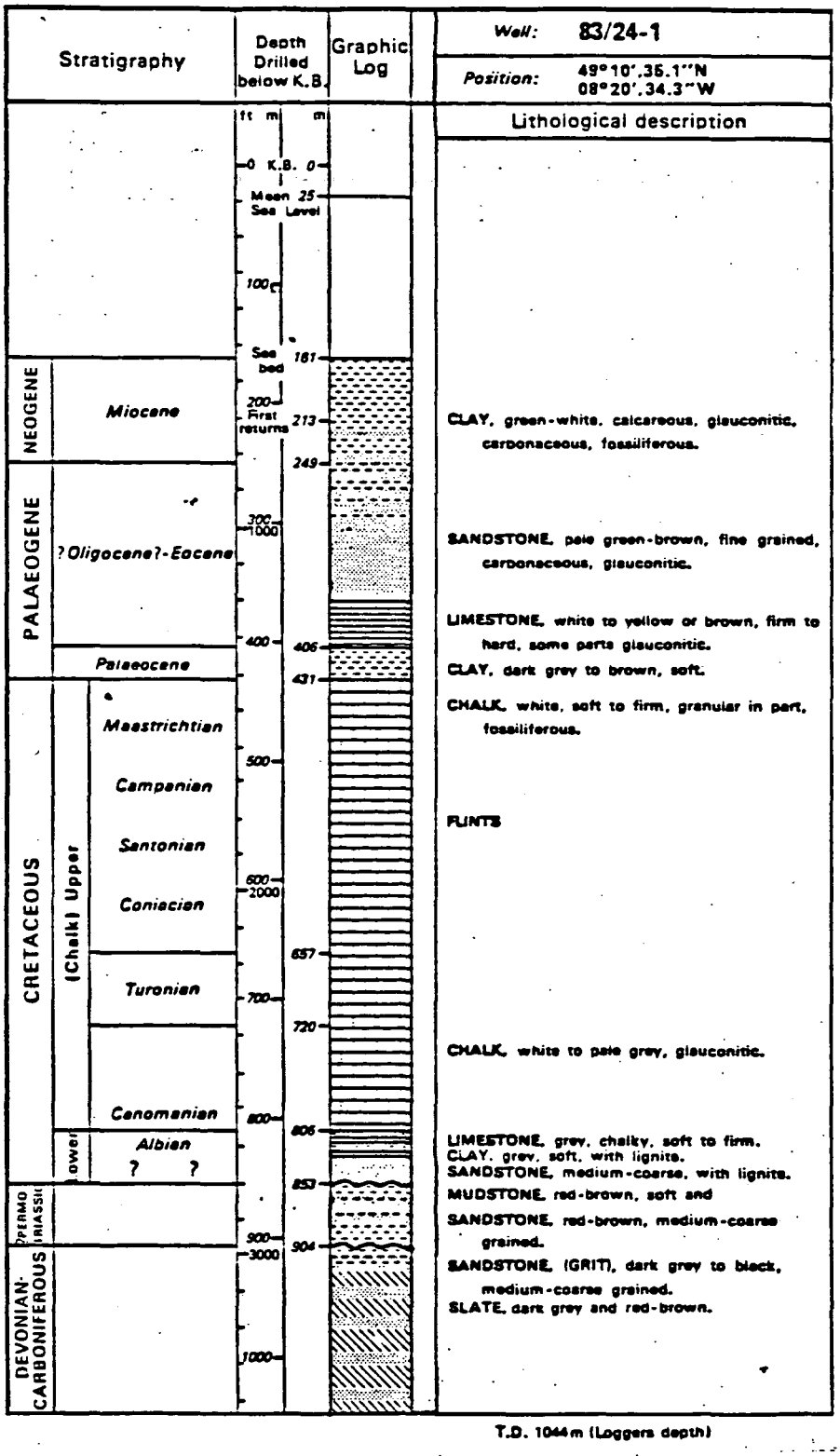

T.D. 1044 m (Loggers depth)

Fig 1.6 Summary of succession in well 86/18-1

Well : 86/18-1 ; 49° 21' 28·67" N

05° 33' 54·85" W

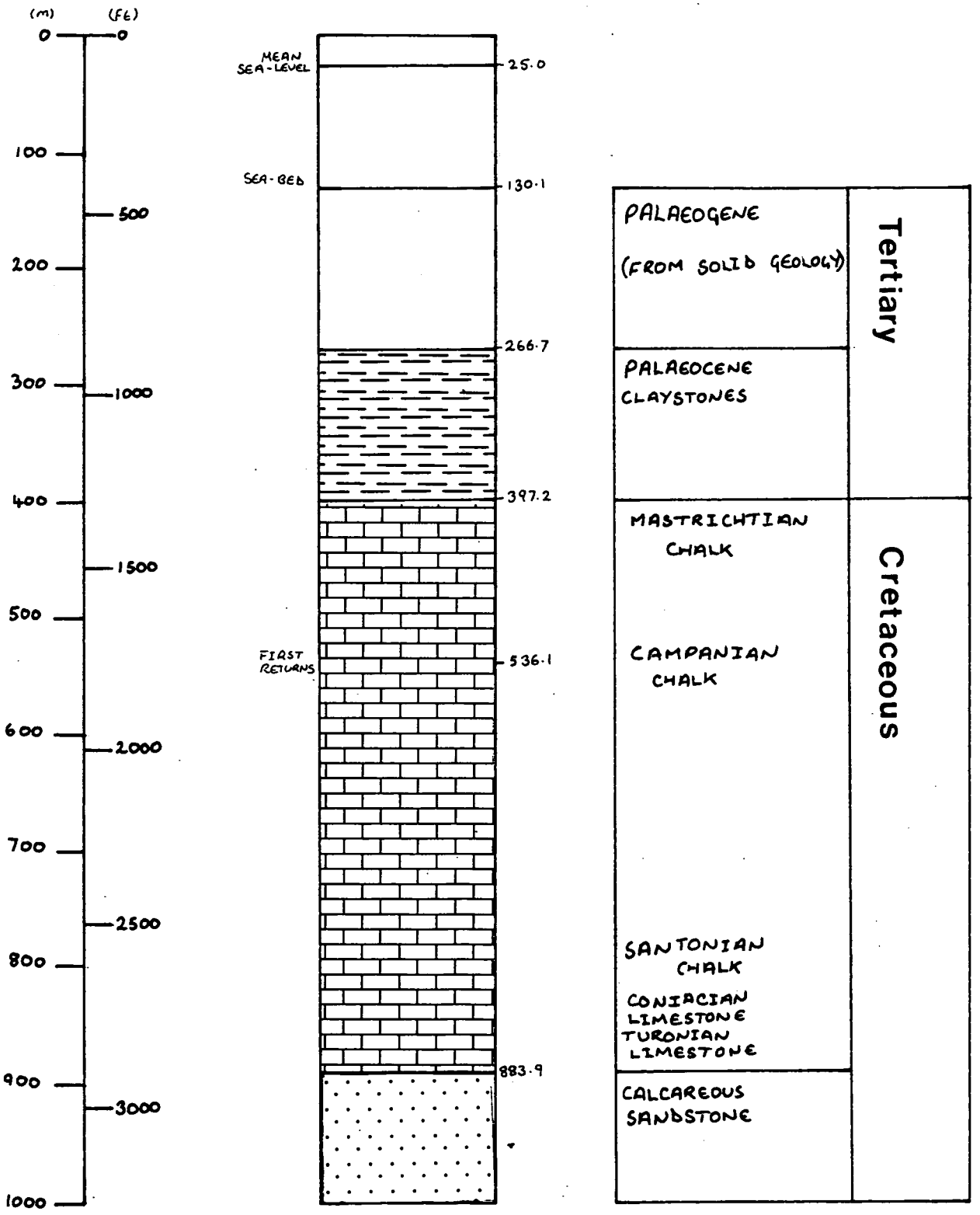

Fig 1.6 (cont.)

Well : 86/18-1 (cont.)

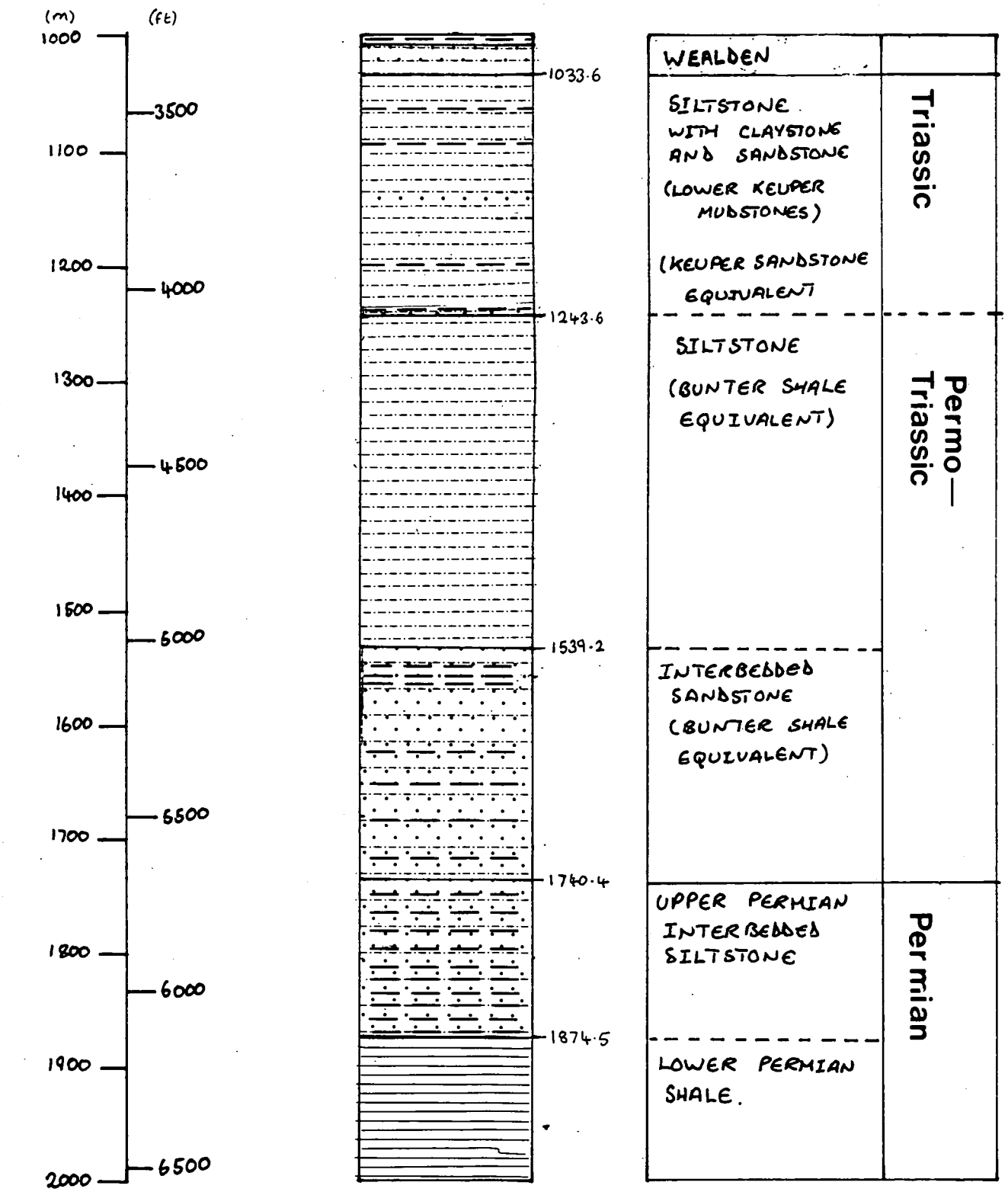

Fig 1.6 (cont.)

Well:86/18-1 (cont.)

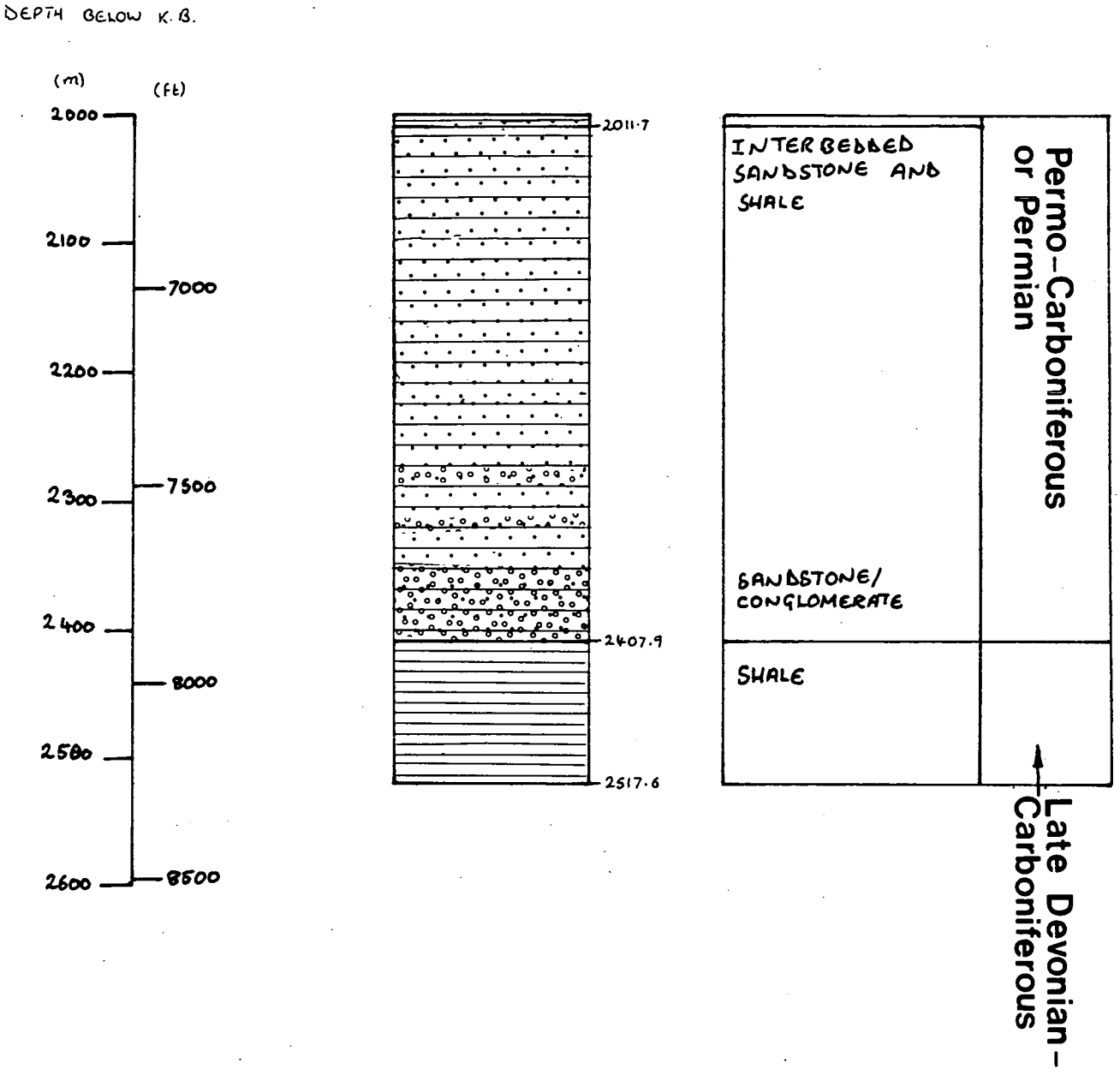

Fig 1.7 Summary of succession in wells 72/10-1 and 72/10-1A

Well: 72/10-1, 72/10-1A

1) 48° 47' 22·85"N, 1A) 48° 47' 23·4"N

09° 06' 01·76"W 09° 06' 01·9"W

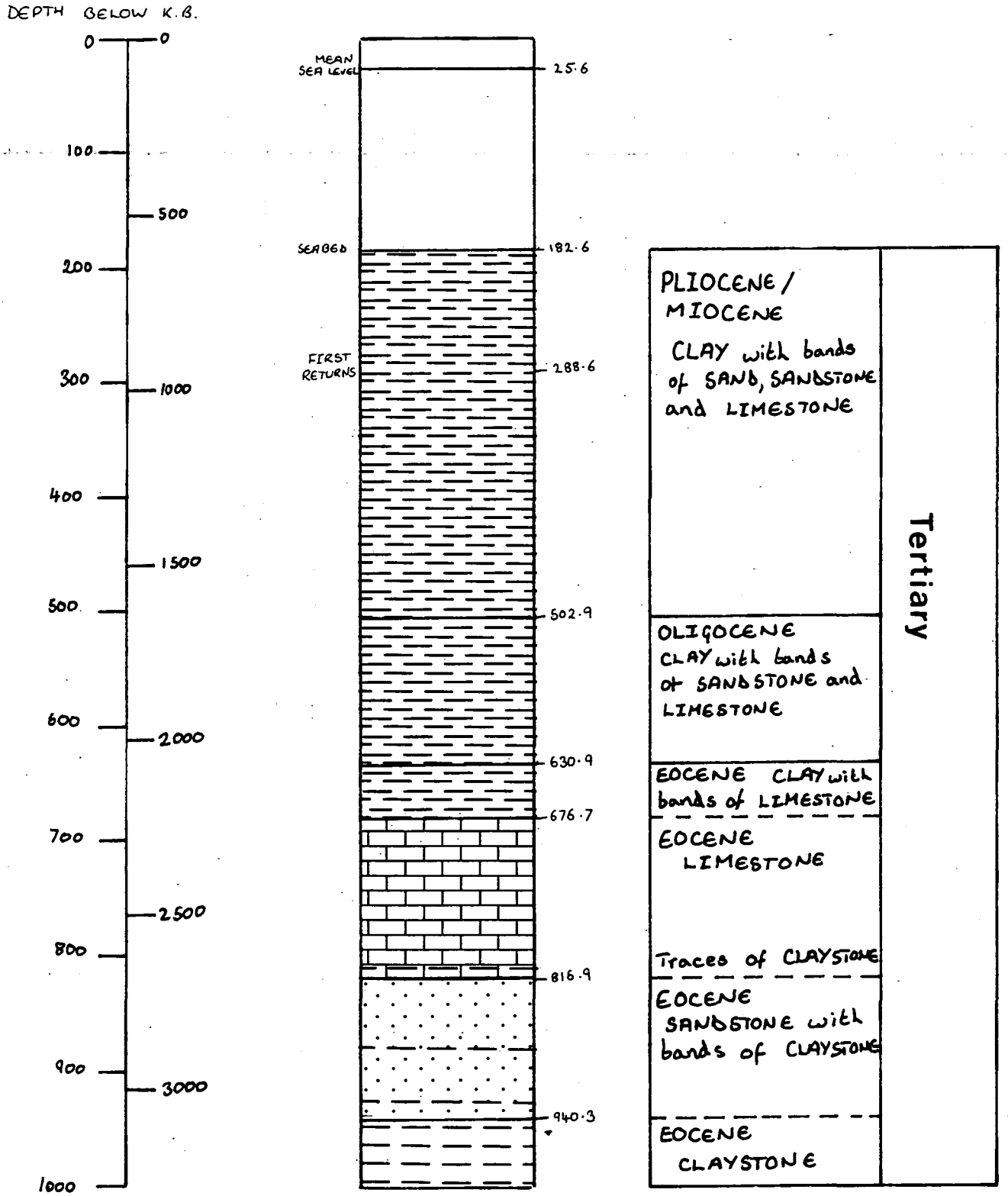

Fig 1.7 (cont.)

Well : 72/10-1, 72/10-1A (cont.)

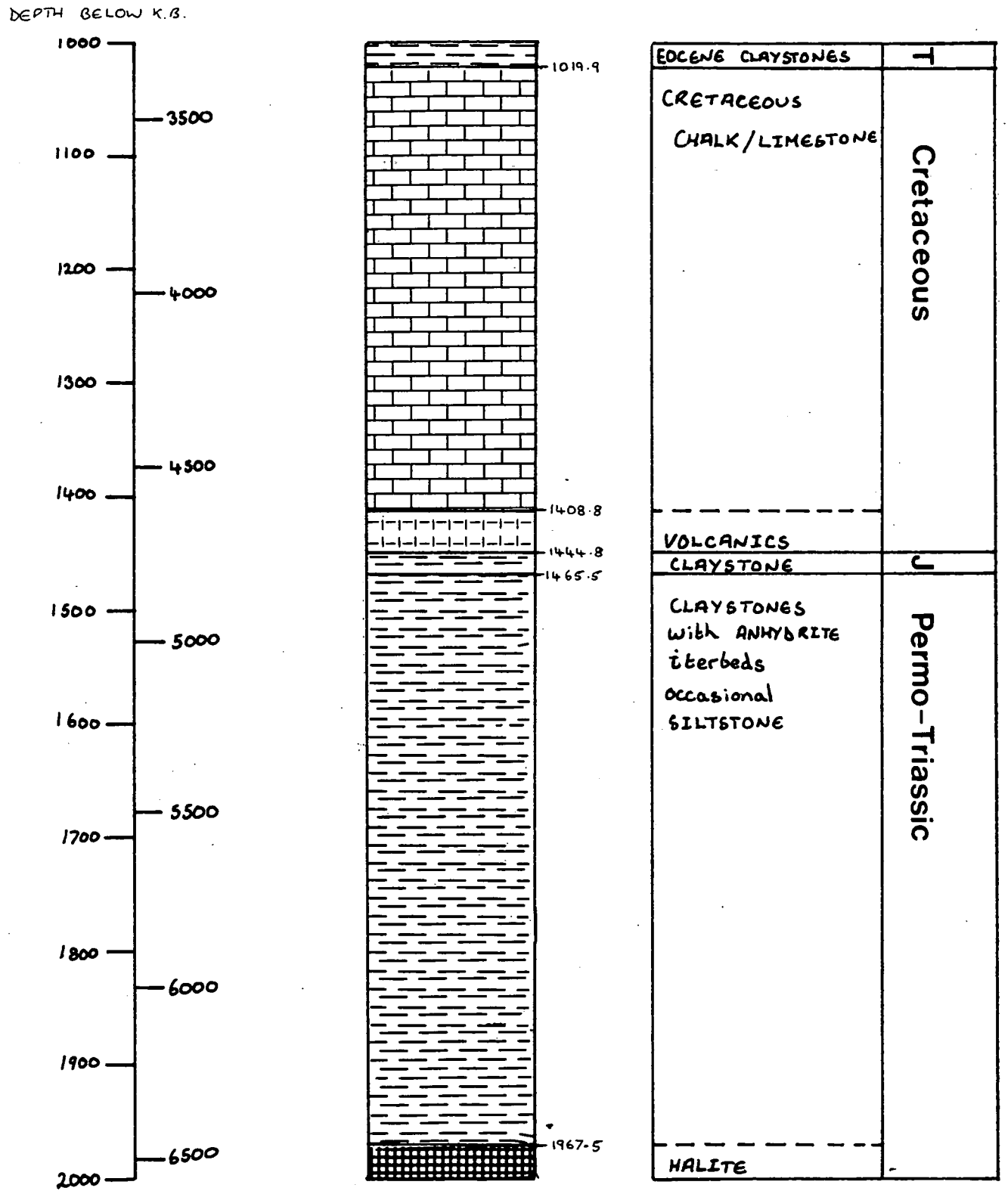

T - Tertiary

J - Jurassic

Fig 1.7 (cont.)

Well: 72/10-1, 72/10-1A (cont.)

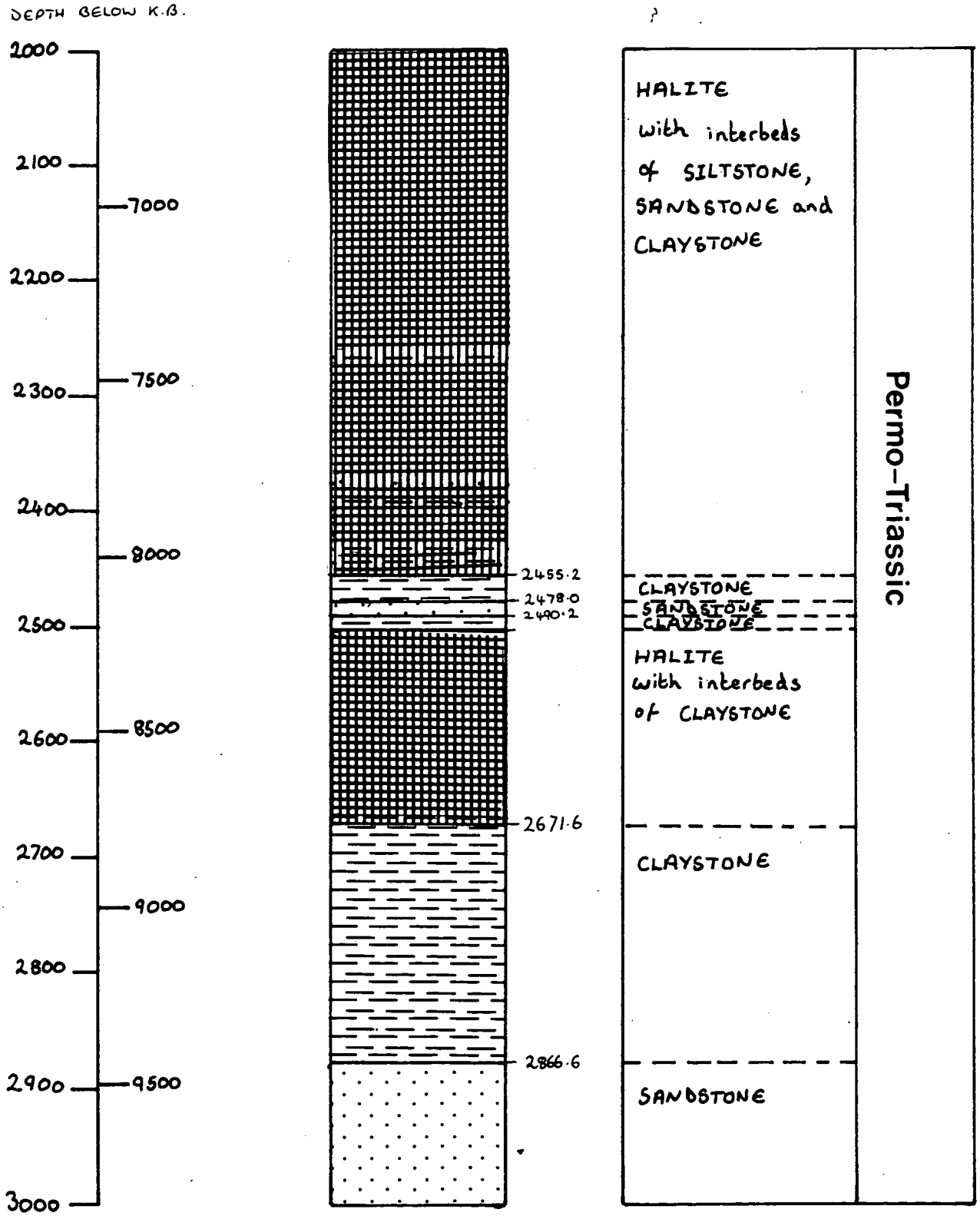

Fig 1.7 (cont.)

Well : 72/10-1, 72/10-1A (cont.)

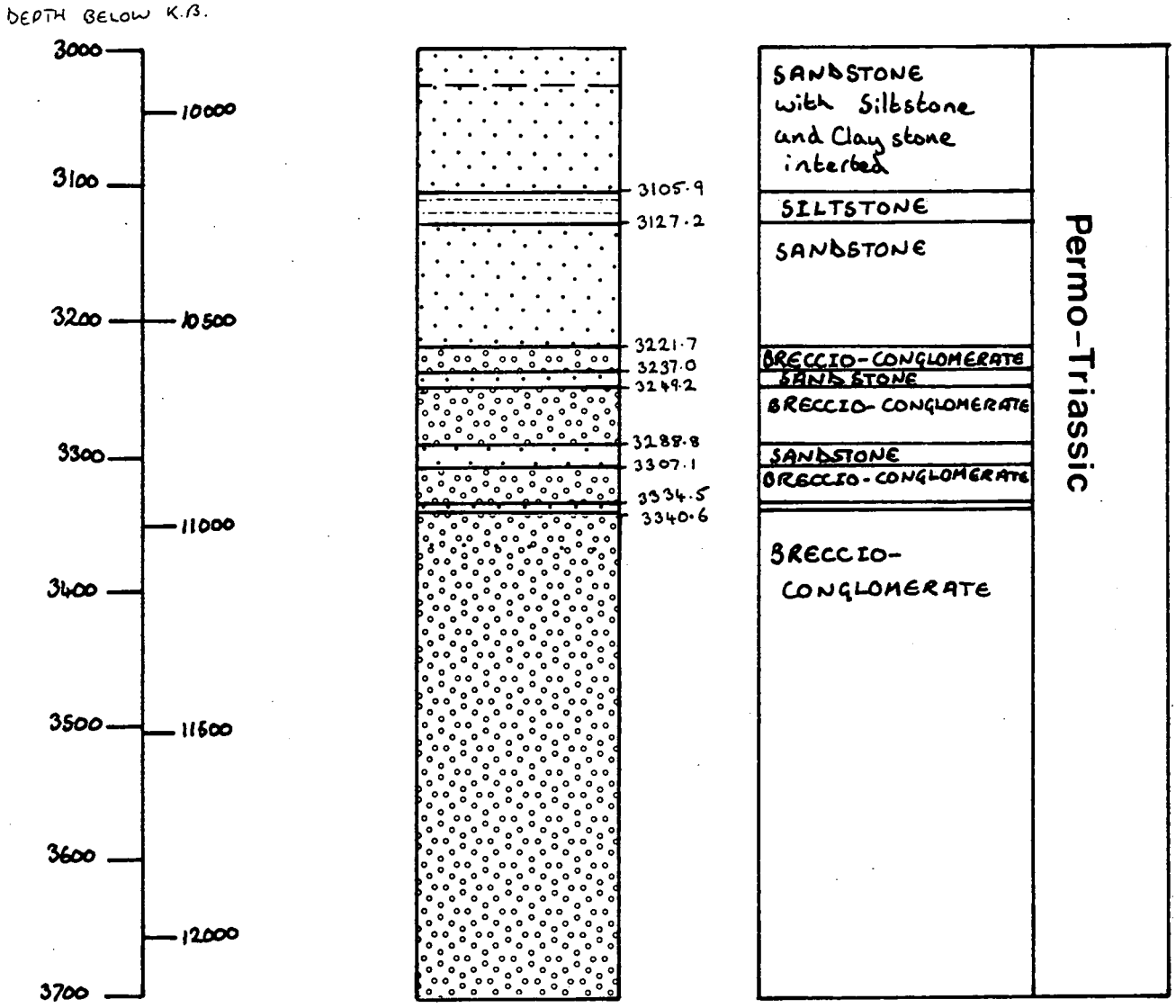

Fig 1.8 Summary of succession in well 87/12-1A

Well: 87/12-1A ; 49° 34' 19·985" N
04° 43' 25·995" W

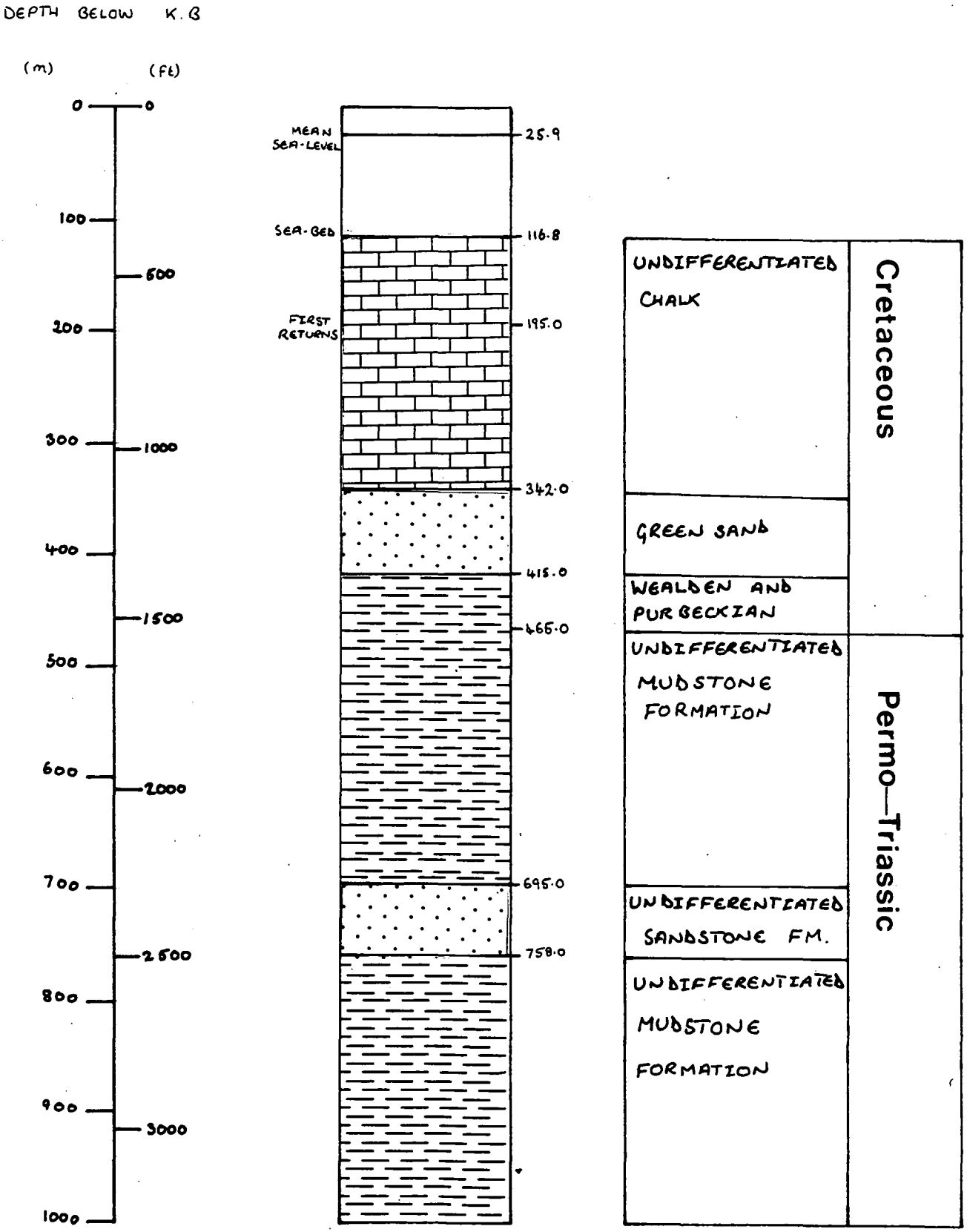

Fig 1.8 (cont.)

Well: 87/12 −1A (cont.)

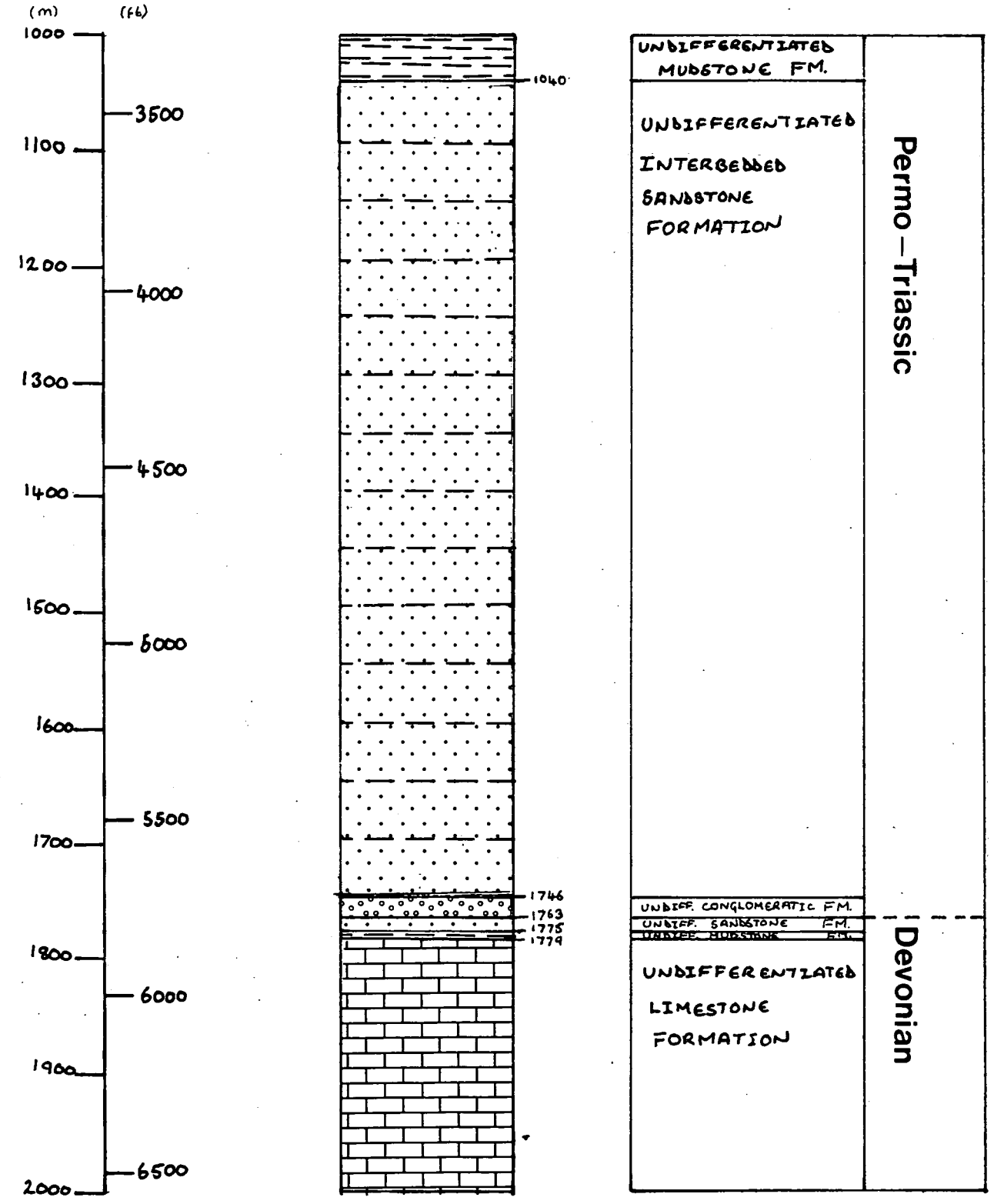

Fig 1.8 (cont.)

Well : 87/12–1A (cont.)

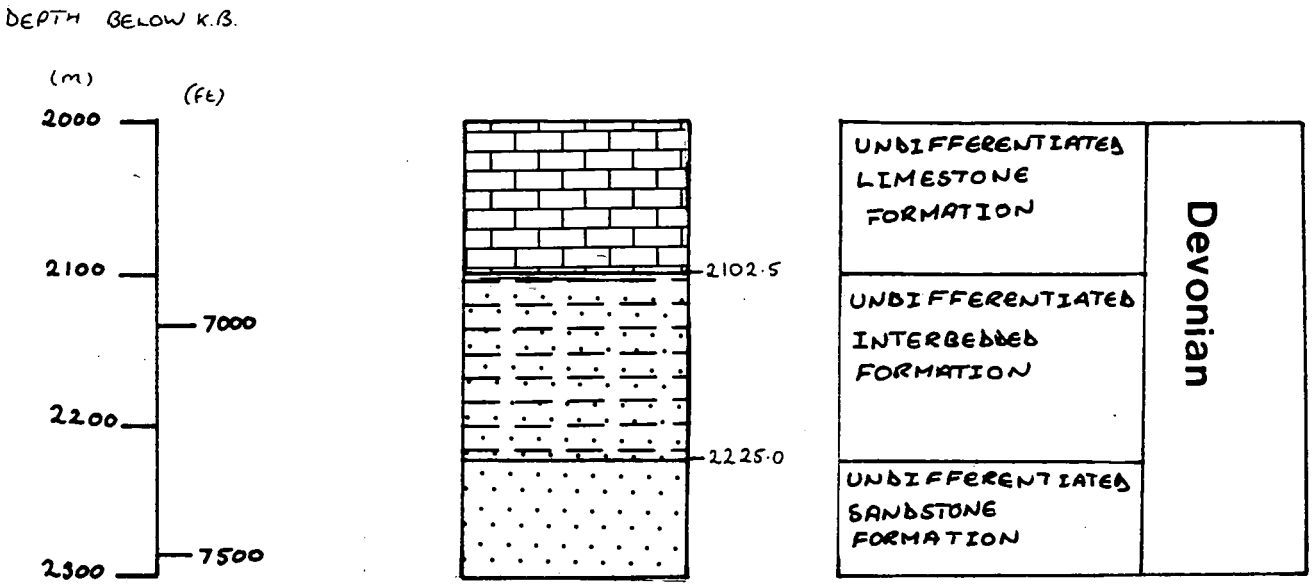

CHAPTER 2

ESTABLISHMENT OF AN ORACLE DATABASE FOR REFRACTION EXPERIMENTS

2 Establishment of an ORACLE Database for Refraction Experiments

A database was required which contained information from refraction experiements in the SWA (South Western Approaches) area. The database was set-up in the form of tables on ORACLE, a VAX utility. The information was separated into two tables - one containing information on each refraction station, and one containing velocity and depth information (Table 2.1).

A detailed description of the data in each column of the tables is shown below.

IDENT - An arbitrary number given to each station for the purpose of linking the two tables.

SOURCE - The name/names of the people from whom the the information was obtained.

S-IDENT - In some cases a station was given an identification number by the source, if this was the case this number is shown.

POSIT - The position of the detector along the shot-line, denoted by a single letter (E = end; C = centre). For a number of stations the position of the detector was unknown and so this column was left blank.

DETECT - Three different types of detector were used in the experiements and are identified in this column as - SB = Sonobuoy; BH = Bottom Hydrophone; BG = Bottom Geophone. Again for a number of stations this information was unavailable and this column was left blank in these cases.

YEAR - The year in which the experiment was carried out.

LAT,LONG - The latitude and longitude of each station. North and East were given positive values, South and West were given negative values.

LINK - The identification number of a station linked with this particular station, with which it makes a reversed shot allowing for calculation of the slopes of the refractors.

DIREC - Direction of each shot from the detector.

COMM - Comments on data and extra details.

PICKED-VEL - The velocity picked for the relevant refractor.

STAND-DIV - The standard deviation in the picked velocity, if it is known.

DEPTH - The estimated depth of the top of the refractor

INTERP - The interpretation of the refractor, based on solid geology maps and the picked velocity.

INDEX-NO - Each successive refractor was given a number to represent its position in the sequence. 1 for the seabed refractor, 2 for the refractor below.

Table 2.1 Tables used in the database

Table 2.1a Station Information

Table name - REFRACTION-DATA

Column Name	Description
IDENT	Identification number
SOURCE	Source of data
S-IDENT	Identification used by source
POSIT	Position of detector on shot line
DETEC	Type of detector used
YEAR	Year when experiment was carried out
LAT	Latitude of station
LON	Longitude of station
LINK	Linked station identification number
DIREC	Direction of shot
COMM	Comments

Table 2.1b Refraction velocities and depths

Table name VELOCITY-DATA

Column Name	Description
IDENT	Identification number
PICKED-VEL	Picked velocity for refractor
STAND-DIV	Standard deviation in velocity
DEPTH	Depth of top of refractor
INTERP	Interpretation
INDEX-NO	Refractor index number
COMM	Comments

The use of various ORACLE commands allow data to be accessed from the tables and calculations and procedures to be performed on them.

Fig 2.1 is an example of such data manipulation, carried out on SAS, a VAX utility for statistical management of data. It shows a plot of the log of the depth against the log of the picked velocity for each refractor. The majority of points lie below a straight line, inferring a relationship between depth and velocity which has been displaced by uplift in much of the area covered.

FIG 2.1 LOG(DEPTH)/LOG(VELOCITY) PLOT FOR REFRACTORS.

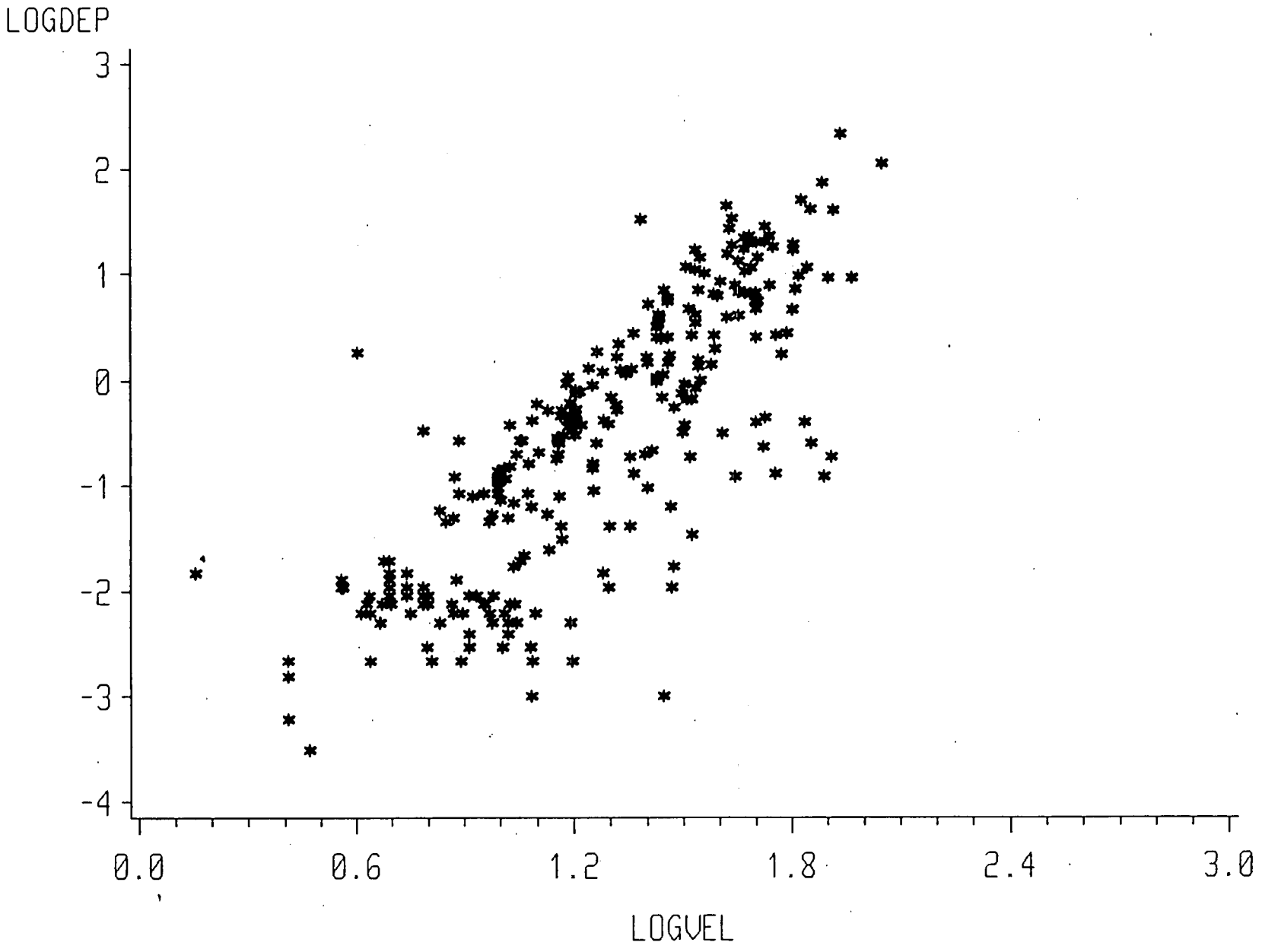

CHAPTER 3

SECTIONS THROUGH THE MELVILLE BASIN

3.1 Introduction

This chapter describes the modelling of the upper Earth's crust along two lines through the Melville Basin. Fig 3.1 shows the location of these lines and demonstrates that they run perpendicular to the general ENE-WSW trend of the surrounding sedimentary basins.

A time section was constructed for each line, using information from two-way-time contour maps of the major reflective horizons held by the Hydrocarbons Research Programme of BGS. The time sections were converted to depth sections using stacking velocities.

Suitable densities and magnetic susceptibilities were assigned to each body in the depth section after consultation of well density logs and tables of typical values (Telford et al, 1976), (Grant and West, 1965). The gravitational and magnetic effects of the models were calculated and compared with the observed anomalies. Using an iterative process between the gravity and magnetic models adjustments were made to gain satisfactory matches between observed and calculated anomalies.

3.2 Brief Geological Description of the Region

The major features of the area are a series of WSW-ENE trending sedimentary basins with boundaries formed by basement highs. The basins were initiated by Permo-Triassic rifting which was later filled in with Permian, Mesozoic and Tertiary sediments.

The basement rocks range from Pre-Cambrian age on the Southern margin of the South-Western Approaches Basin (SWAB) to Devono-Carboniferous sediments and metasediments beneath the other basins (Naylor and Shannon, 1982).

Both sections traverse the well developed local faulting at the northern margin of the Melville Basin, crossing from the Cornubian Platform to the median line. Line A just cuts the Southern margin of the Haig Fras Basin.

The SWAB and Melville Basin are deep, fault bounded structures which to the north of the median line contain a thick Permo-Triassic sequence, overlain by a thin layer of lower Cretaceous sediments and a uniform layer of Cretaceous Chalk. Tertiary material overlays the Chalk and deepens to the south-west of the basin, and small, fault bounded wedges of Jurssic sediments have been observed between the lower Cretaceous and Permo-Triassic layers (Evans et al, 1981). Permian volcanics have been detected in the Melville Basin (well 73/12) and are thought to cover an area corresponding to an extensive magnetic high (Edwards in prep) which is crossed by line B.

The Haig Fras basin is thought to contain Permo-Triassic and possibly Jurassic sediments overlain by a thin layer of Cretaceous Chalk. The Celtic sea basins are not traversed by the sections and so will not be discussed here.

3.3 Models

The sections were modelled using a 2.5D modelling program, GM25DV1 which is described by Busby 1986. The deepest mapped reflective horizon was the top of the basement, about 8 km deep at the deepest point. The model was given a depth of 12 km, the approximate depth of a zone of near horizontal, discontinuous reflectors within the basement rock seen on BIRPS SWAT lines 5, 6 and 7 (Privé, 1987). The top of this zone lies at depths between 10 and 14 km.

3.4 Gravity Modelling

After suitable densities were assigned to the bodies in the models, each model was given a background density which gave calculated anomalies of similar amplitude to those observed. Table 3.1 shows all the density values used in the models.

To prevent the calculated anomalies dropping to zero at the ends of the modelled sections, the upper crustal layers were extended horizontally for 50 km to the NW and SE of the sections to give a mass representative of the surrounding rocks. This was not completely satisfactory but consultation of depth contour, (Smith, 1985) and geology (Evans, 1982, 1985) maps of the area showed there were no bodies likely to have a large effect on the observed anomaly within 50 km of the sections. Similar considerations were used in determining the half-strike length of the bodies in the models, all the bodies in the sections, with the exception of the Jurassic wedges and Triassic salt, extend over the entire basin. As the Jurassic material has a similar density to the Triassic layer, the adjustment of the half-strike lengths of these bodies made negligible difference to the calculated anomaly. The Triassic salt body is responsible for the gravitational lows at the centre of each section and so variations in its half-strike length will have an effect on the calculated anomaly. Study of the gravitational low resulting from the presence of the salt in Bouguer anomaly maps (Abraham, in prep) showed an extension of at least 25 km to either side of the sections, and so this value was used as the half-strike length of the salt.

When the basement was modelled as a body of uniform density there was a discrepancy between observed and calculated anomalies to the south of each section. This was eliminated by dividing the basement in to two bodies of differing density along a near-vertical fault at the northern margin of the Melville Basin. The basement to the north of the Melville Basin is known to consist mainly of slates and sandstones, well 83/24 (Fig 3.1) penetrates this material at a depth of 827m. The slate is less dense than the southern basement material (Table 3.1).

3.5 Magnetic Modelling

After assigning suitable susceptibilities to each body in a magnetic field of 37.9 A/m, and subtracting a regional field from the observed to give a residual anomaly, an acceptable match between observed and calculated anomalies in each section was not obtained.

The pick for the Permian lava/Basement horizon on the seismic line B was uncertain and so extensive adjustments to the shape and size of the Permian lava body along this horizon were permitted. This enabled an acceptable fit to be obtained near the centre and to the south of the section (Fig 3.2) on a 'trial and error' basis. It was necessary to insert a small body of high magnetic susceptibility between the Permo-Triassic and Basement bodies in line A to produce the required magnetic anomaly. Although no evidence for this body is seen on the seismic lines it is possible that any signal associated with it was obscured by the signal from the top of the Basement. The body was given the same magnetic susceptibility as the Permian lava body in section line B and is assumed to consist of the same material. Fig 3.3 shows the position of this body.

The regional field subtracted from observed field to give the residual field for each section was 700 gammas. Table 3.2 shows the susceptibilities.

3.6 Conclusions

Gravity and magnetic models along lines A and B were produced which showed acceptable fits between observed and calculated anomalies.

A discrepancy between observed and calculated gravity anomalies to the south of each modelled section was eliminated by bisecting the Basement along a near-vertical fault at the northern margin of the Melville Basin. The two halves were assigned differing densities the less dense material to the north.

Table 3.1 Densities used in Models

Interpreted Body	Density (gm/cm^3)	
	Line A	Line B
Sea	1.03	1.03
Tertiary	2.00	2.00
Chalk	2.20	2.20
Jurassic	2.45	2.45
Triassic Salt	2.05	2.05
Triassic	2.50/2.47	2.50
Permo-Triassic	2.58	2.58
Permian volcanics	2.70	2.70
Northern Basement	2.60	2.58
Southern Basement	2.67	2.67
Background	2.471	2.448

Table 3.2 Magnetic Susceptibilities used in Models

Interpreted Body	Magnetic Susceptibility	
	Line A	Line B
Sea	0	0
Tertiary	0.339×10^{-3}	0.339×10^{-3}
Chalk	0.314×10^{-3}	0.314×10^{-3}
Jurassic	0.377×10^{-2}	0.377×10^{-2}
Triassic Salt	0	0
Triassic	0.377×10^{-2}	0.377×10^{-2}
Permo-Triassic	0.377×10^{-2}	0.377×10^{-2}
Permian Volcanics	0.126	0.126
Northern Basement	0.628×10^{-2}	0.628×10^{-2}
Southern Basement	0.628×10^{-2}	0.628×10^{-2}

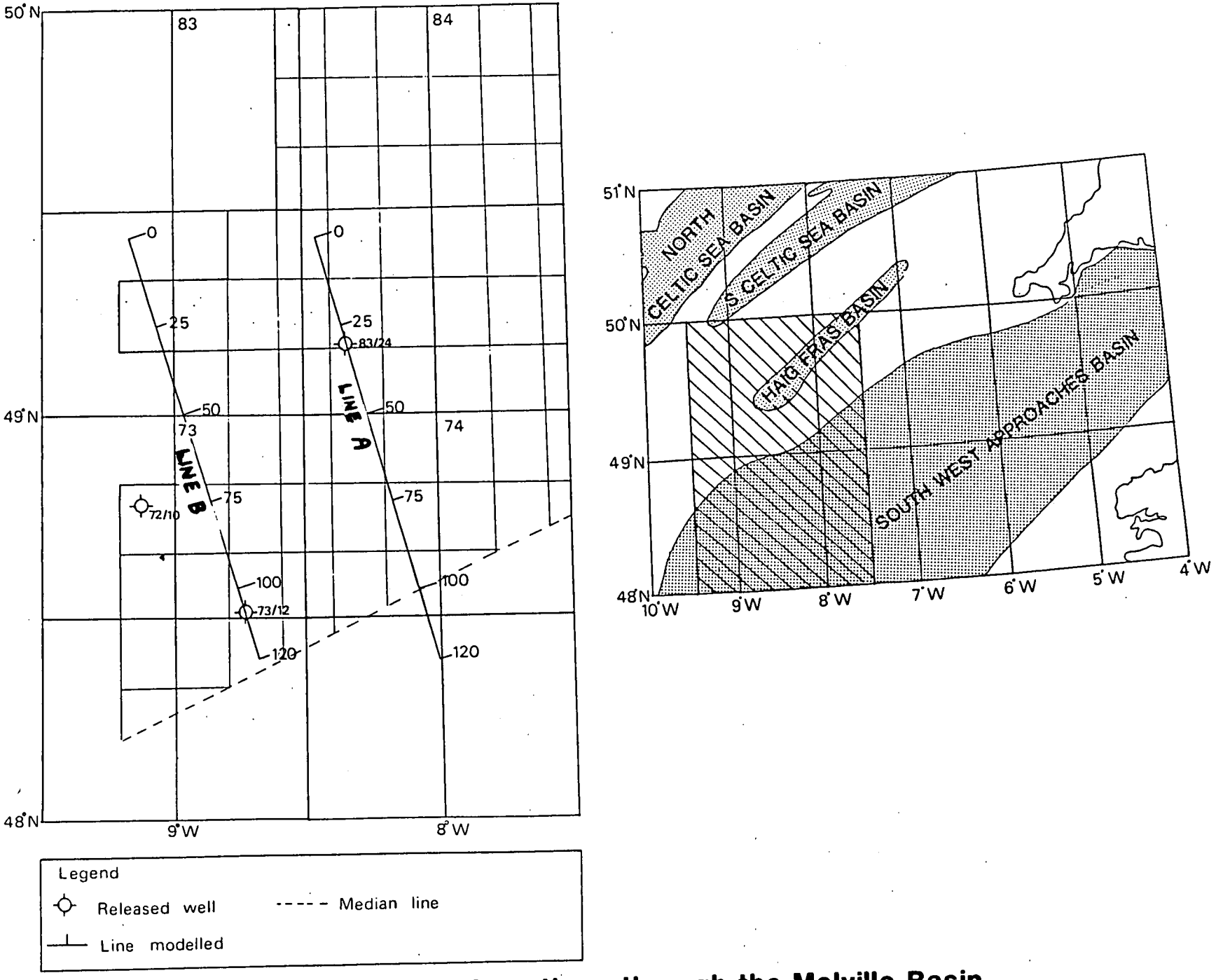

Fig 3.1 Location of sections through the Melville Basin

Fig 3.2 Line B

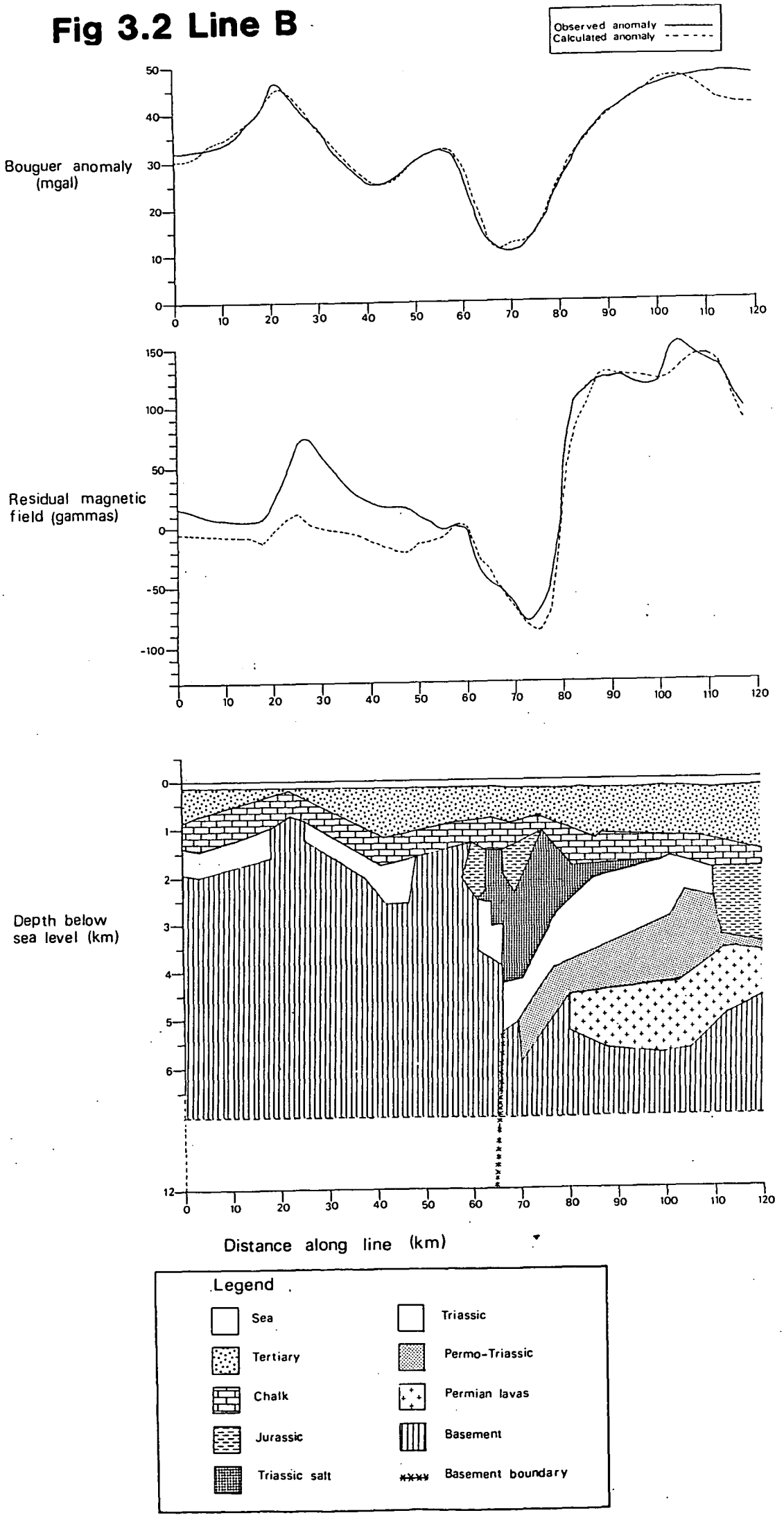
Observed anomaly
Calculated anomaly
Bouguer anomaly (mgal)
50
40
30
20
10
0
0 10 20 30 40 50 60 70 80 90 100 110 120
Residual magnetic field (gammas)
150
100
50
0
-50
-100
0 10 20 30 40 50 60 70 80 90 100 110 120
Depth below sea level (km)
0
1
2
3
4
5
6
12
0 10 20 30 40 50 60 70 80 90 100 110 120
Distance along line (km)
Legend
Sea
Tertiary
Chalk
Jurassic
Triassic salt
Triassic
Permo-Triassic
Permian lavas
Basement
Basement boundary

Fig 3.3 Line A

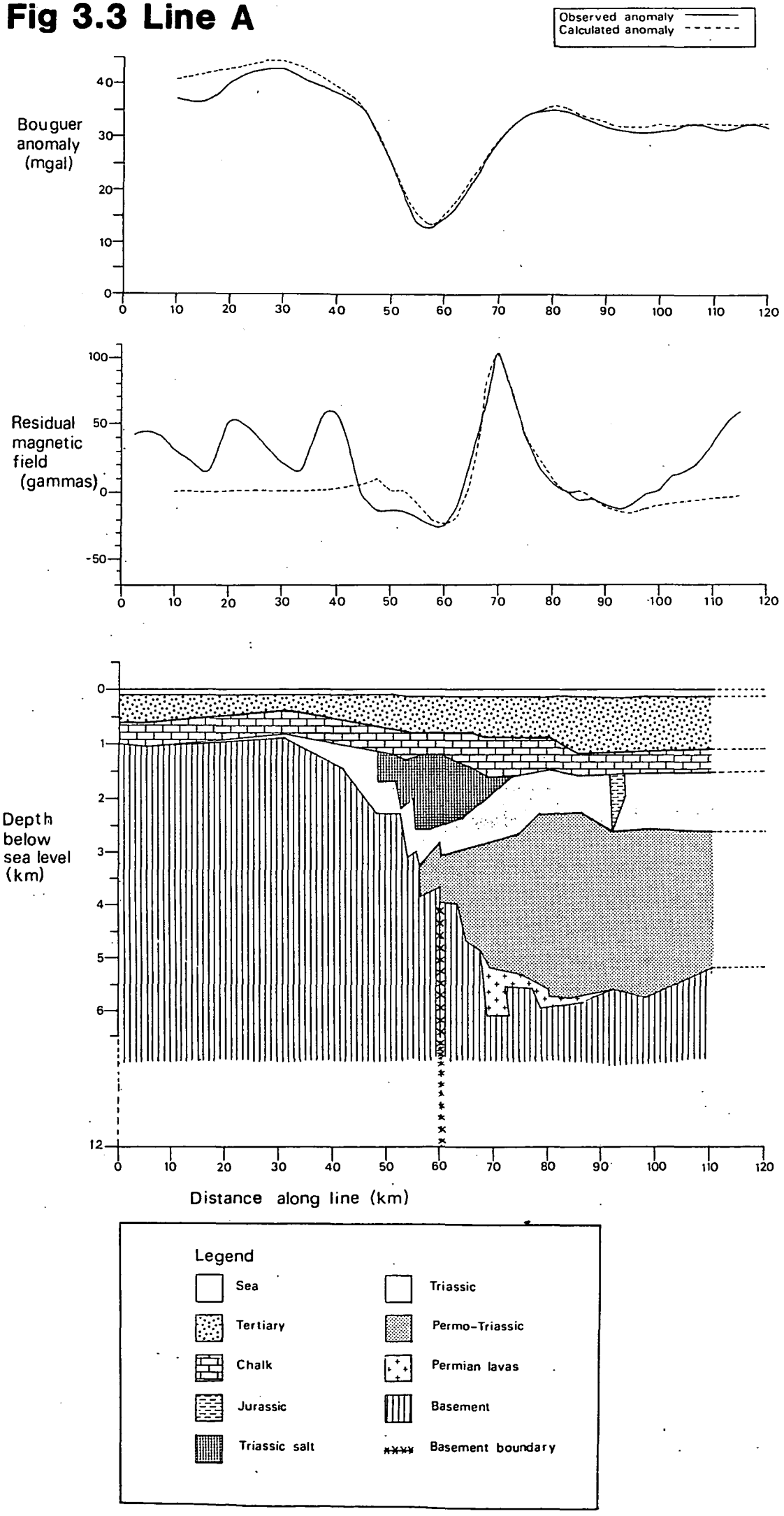
Observed anomaly
Calculated anomaly
Bouguer anomaly (mgal)
40
30
20
10
0
0 10 20 30 40 50 60 70 80 90 100 110 120
Residual magnetic field (gammas)
100
50
0
-50
0 10 20 30 40 50 60 70 80 90 100 110 120
Depth below sea level (km)
0
1
2
3
4
5
6
12
0 10 20 30 40 50 60 70 80 90 100 110 120
Distance along line (km)
Legend
Sea
Tertiary
Chalk
Jurassic
Triassic salt
Triassic
Permo-Triassic
Permian lavas
Basement
Basement boundary

CHAPTER 4

MAGNETIC MODELLING OF THE HAIG FRAS ANOMALY

4.1 Introduction

This chapter contains a summary of the work carried out on the modelling of the Haig Fras magnetic anomaly. The modelling and geological considerations are described in detail in Edwards et al, unpublished.

Marine magnetic surveys in the Celtic Sea area show a magnetic anomaly approximately 56 km long on the north margin of the Haig Fras granite batholith. 30 km of this anomaly can be identified with a high degree of certainty, but the remaining 18 km to the NE and 8 km to the SW were detected with less certainty.

Fig 4.1 shows the position of the batholith in relation to important geological features and known igneous centres.

Fig 4.2 shows the trend of the centre of the magnetic anomaly in relation to the outline of the granite batholith, Bouguer gravity anomaly contours and relevant survey lines. The outline of the batholith was inferred from a 1985 radiometric map, produced by Miller, Roberts and Jones.

Of the survey lines traversing the anomaly the largest magnetic anomaly observed was on line 32 (Fig 4.3) and so this line was modelled. Fig 4.3 also shows the seabed profile along each survey line, the area of the granite outcrop can be identified by the characteristic rough topography. The profiles for lines 31, 32 and 15 also show ridges corresponding to the position of the anomaly. The anomaly was thus assumed to be caused by basic dykes containing natural remanent magnetisation represented by these ridges.

Fig 4.4 shows a single channel sparker record along line 32, the rough topography again indicates the area of granite outcrop and a series of ridges marked D show the position of the dyke. The lack of structure below the seabed reflection between fix numbers 24 and 43 of the record shows the position of the granite batholith, and to the SE a sand wave can be seen above layers of Post-Carboniferous strata.

The Earth's magnetic field in the area has declination and inclination 350° and 67° respectively and a magnitude of 37.9 A/m. A regional field, shown in Fig 4.3, was subtracted from the observed field to give the residual field shown in Fig 4.5.

4.2 Modelling

The modelling was carried out using an interactive magnetic and gravity modelling program, MAGRAV (Walker, 1981).

Initially to determine the total magnetisation associated with the observed anomaly, it was modelled as a single, vertical, 1.5m wide, outcropping dyke. It was assumed that the azimuth of the total magnetisation was either 180° or 0°, (180° for reversed magnetisation and 0° for normal magnetisation). The magnetisation intensity was set to 0.5A/m which gave a calculated anomaly of suitable magnitude, the inclination was varied through 360° at 45° intervals. It was found that the best fit to the observed anomaly occurred for an inclination between 0° and -45° with reversed total magnetisation, (an azimuth of 180°). Further experimentation within these boundaries showed that the most satisfactory model to the observed anomaly, using a single dyke model, was for an inclination of -30° with reversed total magnetisation (Fig 4.7).

The flanks of the calculated anomaly were not as sharply defined as those of the observed anomaly (Fig 4.8), this was common to all the models consisting of dykes solely of reversed magnetisation. It was found that a closer match to the observed anomaly could be obtained by adding normally magnetised dykes to the dyke set. Fig 4.9 shows another model with a normally magnetised dyke at the SE flank of the anomaly and the resultant calculated anomaly, the SE flank of the calculated anomaly matches that of the observed anomaly more closely than previously (Fig 4.8).

Considering this further modelling was carried out using both reversed and normally magnetised dykes and in this way the most satisfactory match was obtained (Fig 4.5) which was 6 dykes, each between 0.13 and 0.42 km wide and between 1 and 10 km deep.

The inclination interpreted of 30° to 65° (Fig 4.6) suggested Mesozoic or Tertiary origin, but the trend of known Tertiary dykes in the area is NW-SE (Kirton et al, 1985) perpendicular to the trend of the modelled dykes. Structural trends in the area demonstrated by the Mesozoic sedimentary basins (Fig 4.1) suggest a Mesozoic origin, as the dyke set follows the same NE-SW trend.

A,Anglesey ADS,Anglesey Dyke Swarm
BAD,Bartestree Dyke BRD,Brockhill Dyke
BSD,Butterton Swynnerton Dyke
CT,Crediton Trough ES,Epson Shoal
EVS,Exeter Volcanic Series F,Finistere
FB,Fastnet Basin
GAR,Grinshill & Acton Reynold Dyke
HFB,Haig Fras Batholith
L,Lundy Igneous Complex
MD,Mathry Dyke
SWI,South West Ireland Dyke System
T,Tregourois WR,Wolf Rock

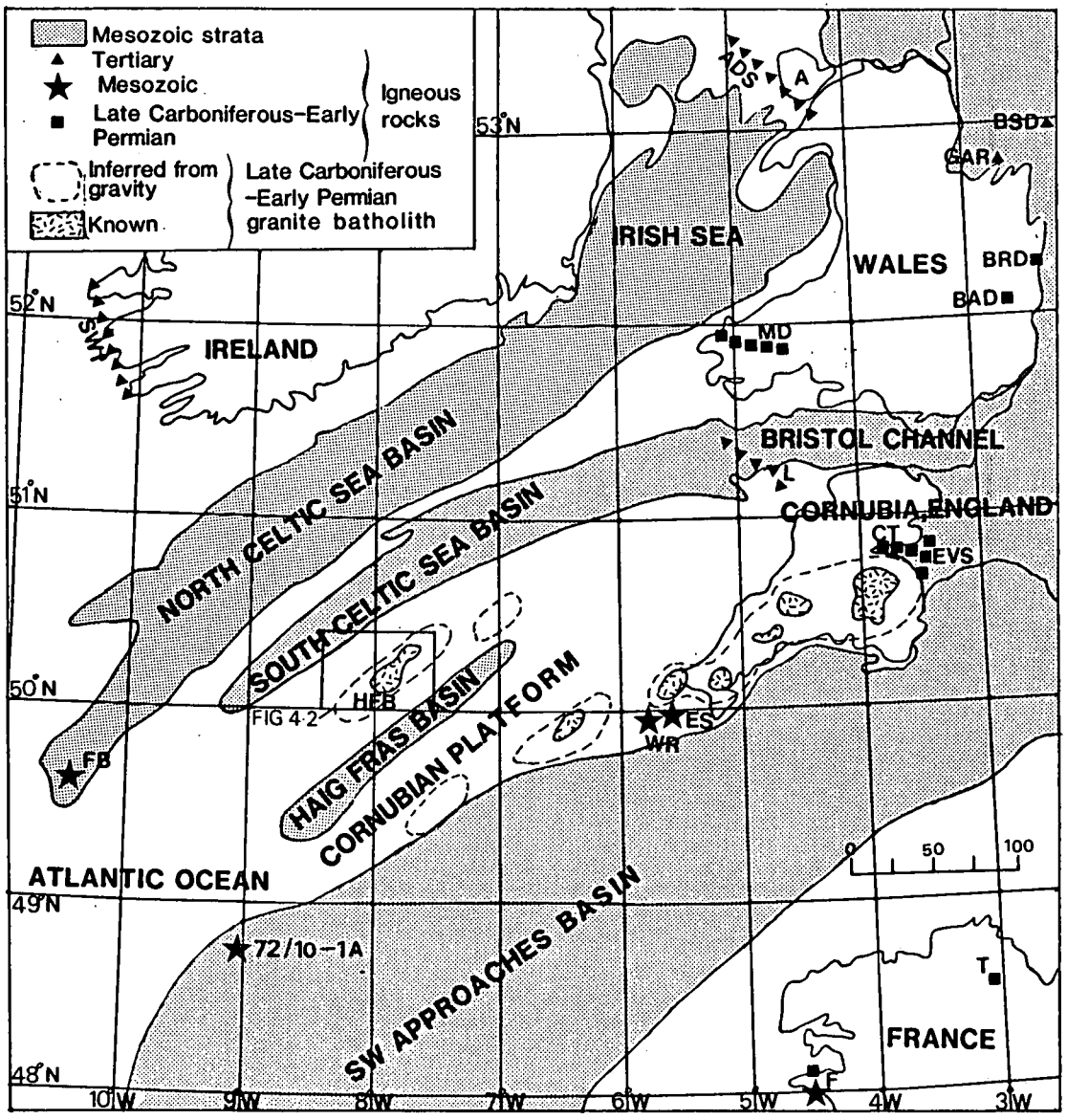

Fig 4.1 Regional setting of Haig Fras area

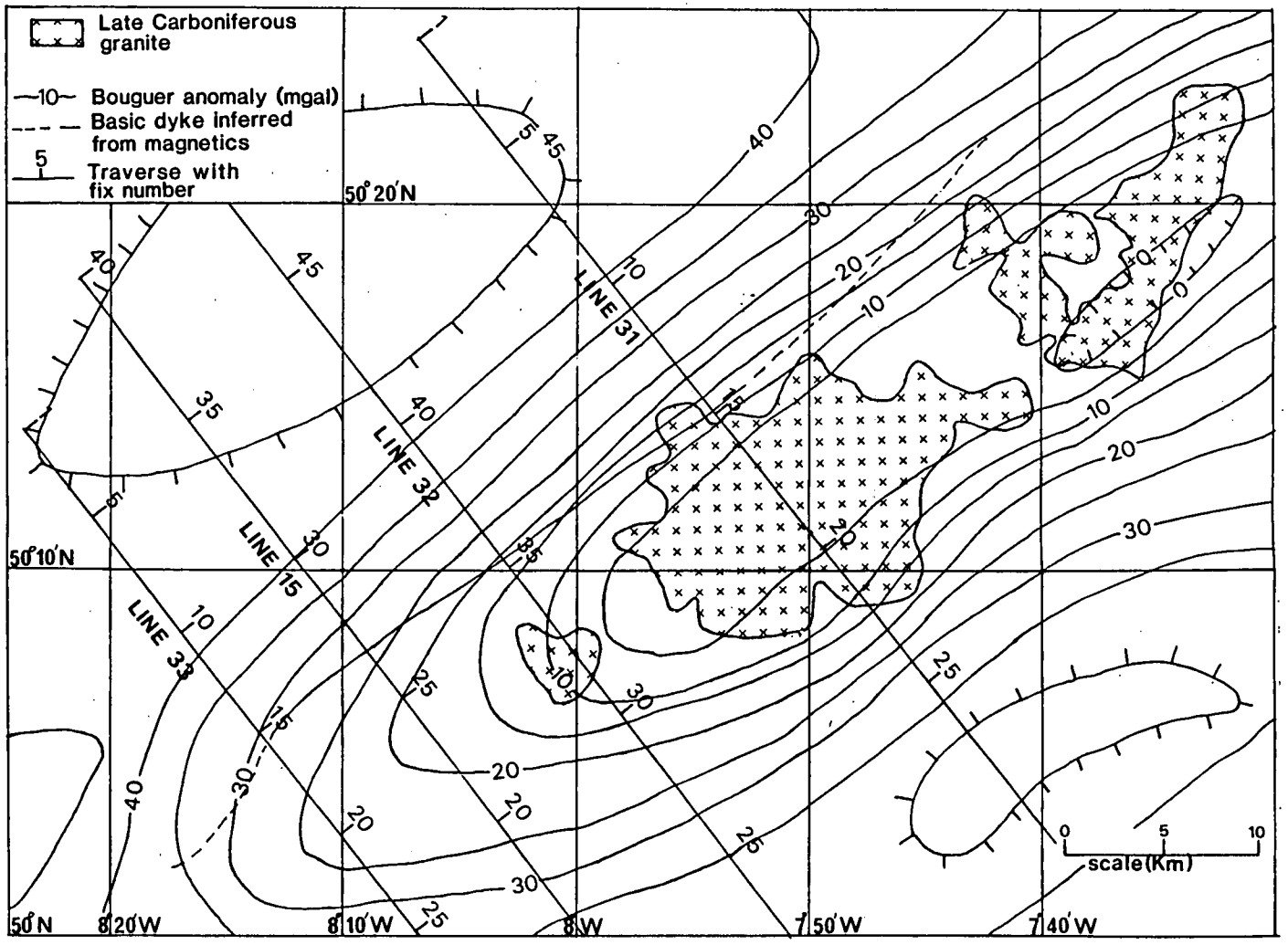

Fig 4.2 Bouguer anomaly map,geophysical traverses and inferred path of basic dyke set,Haig Fras Granite area

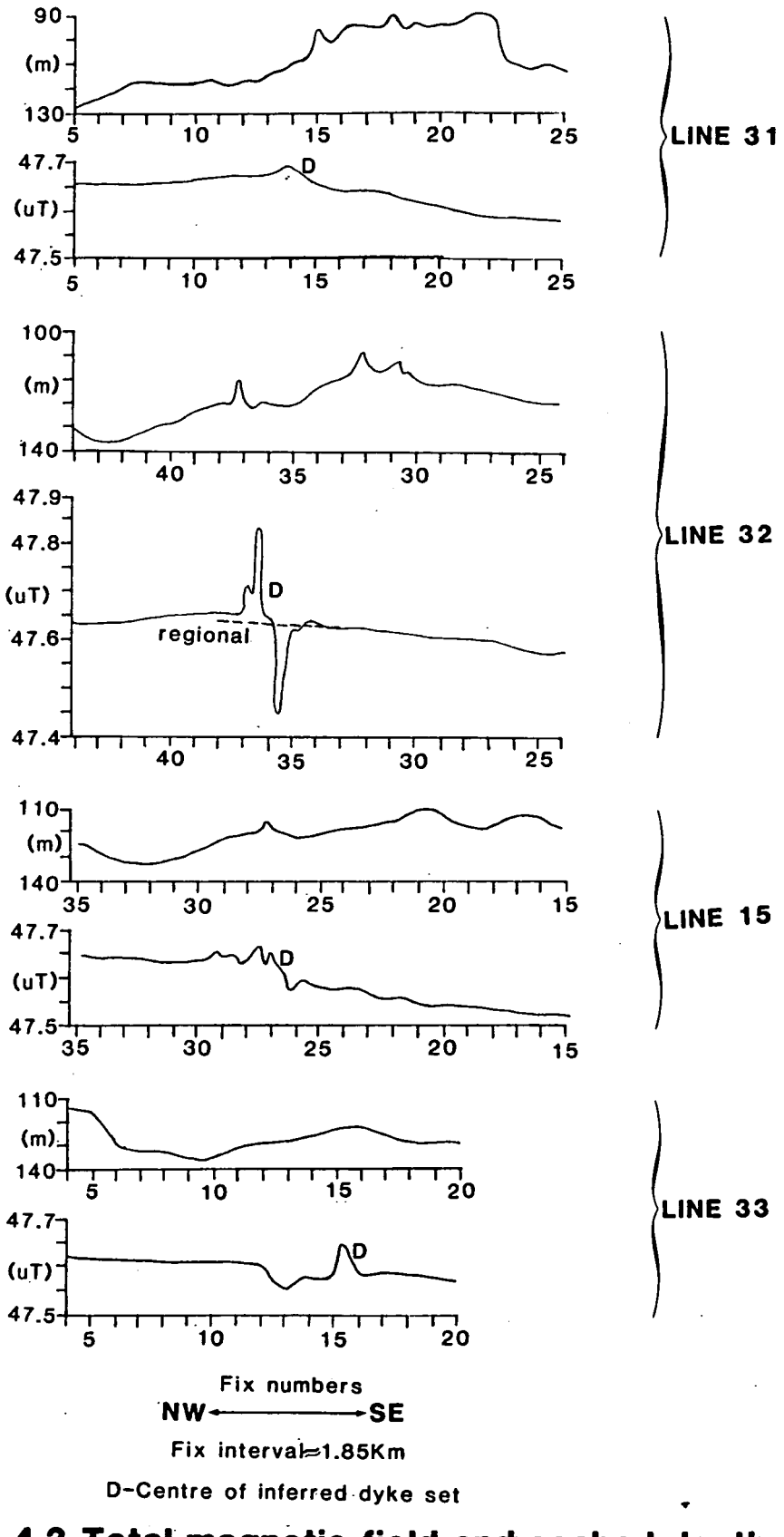

Fig 4.3 Total magnetic field and seabed depth profiles,Haig Fras Granite area

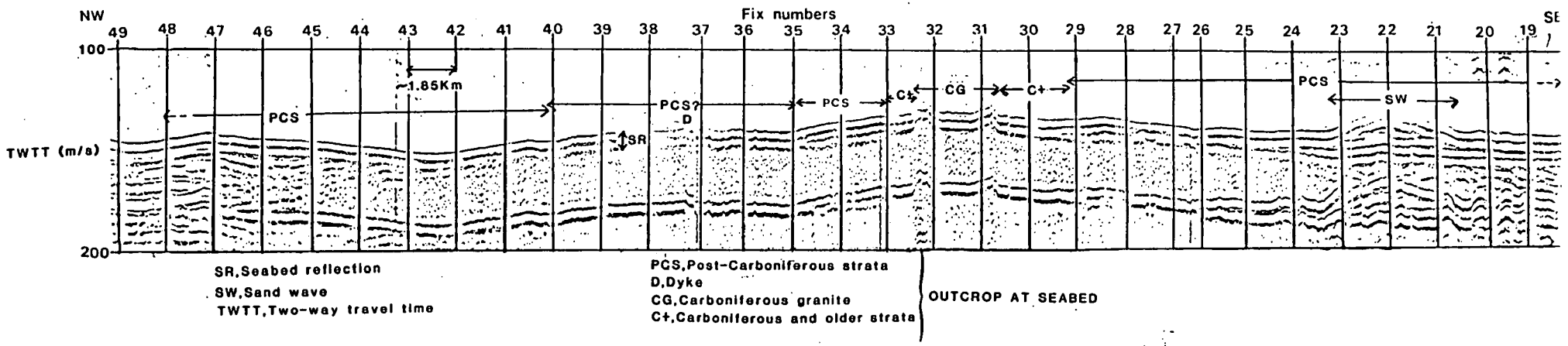

Fig 4.4 Single channel seismic record,Line 32,Haig Fras Granite area

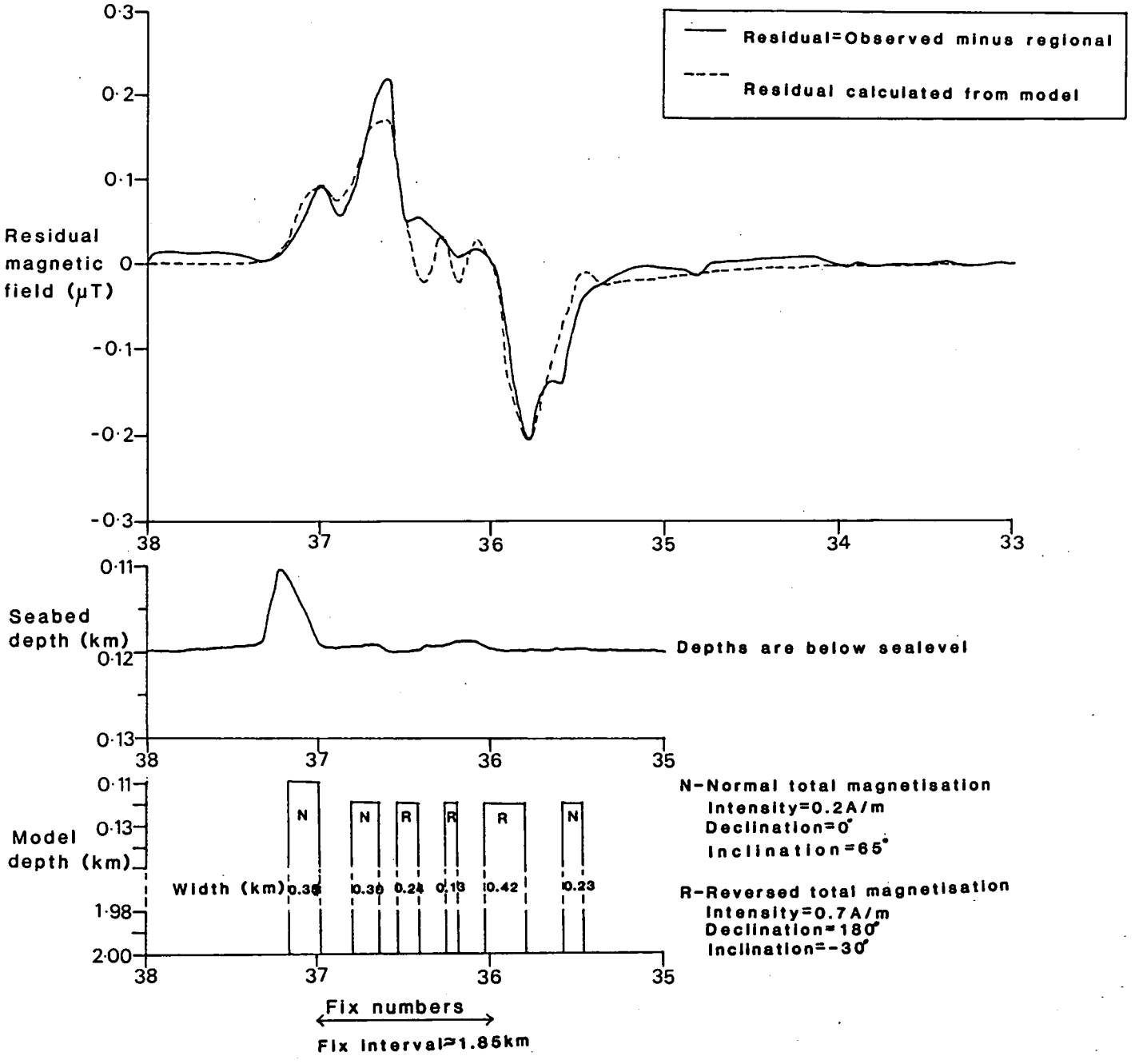

Fig 4.5 Residual magnetic anomaly,seabed depth profile and dyke models,Line 32,Haig Fras area

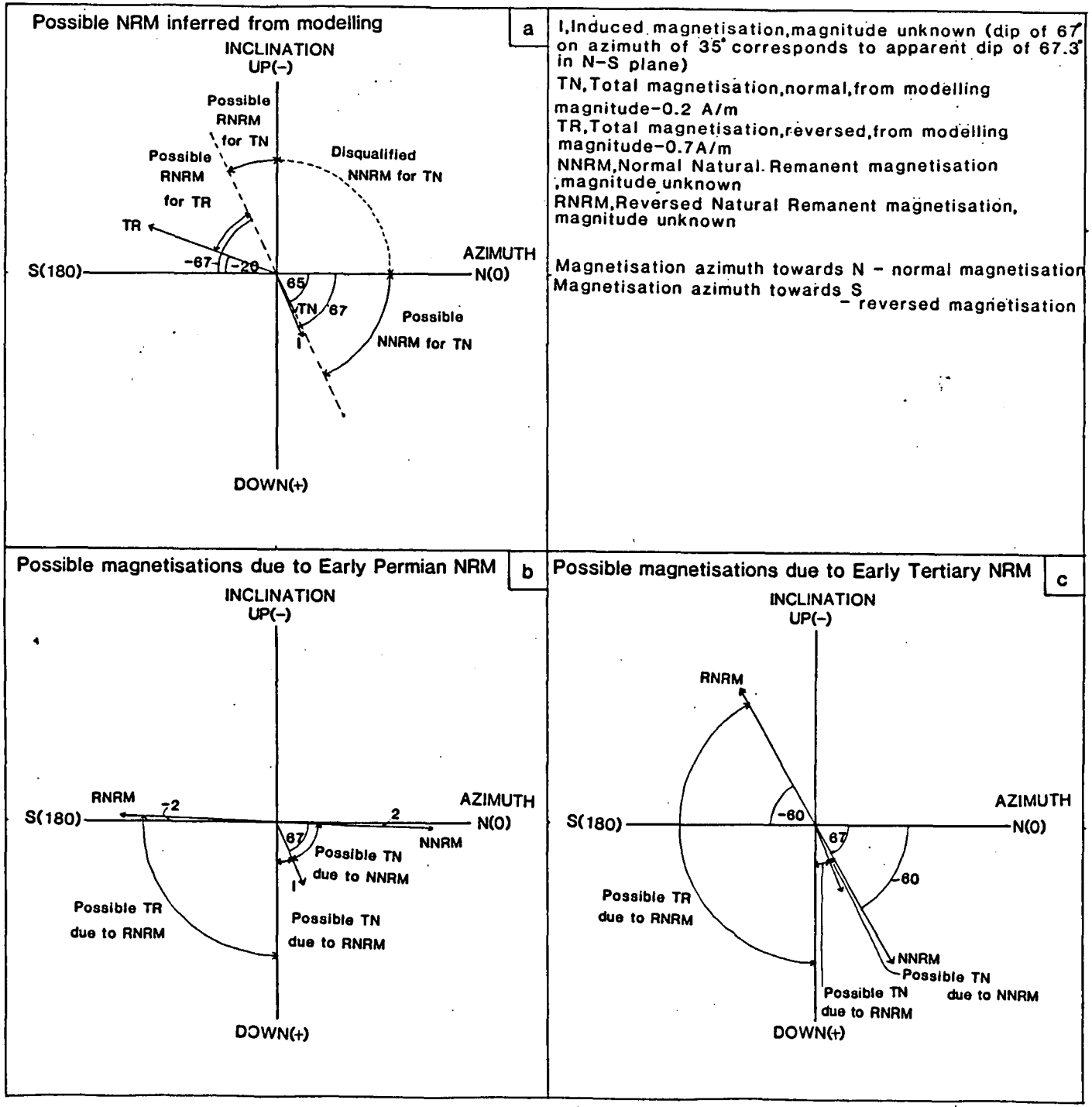

Fig 4.6 Known and possible induced,total and remanent magnetisations,Haig Fras Dyke

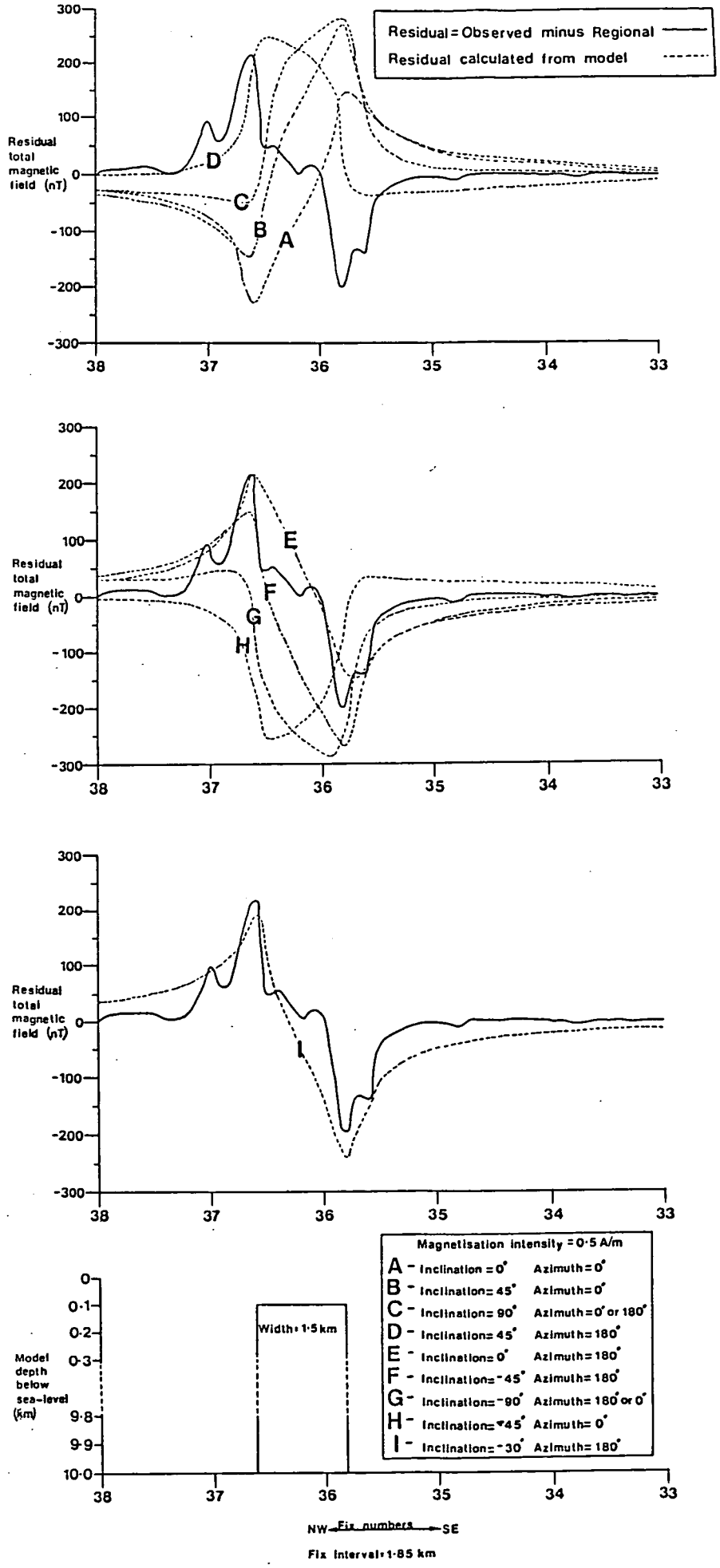

Fig 4.7 Calculated residual magnetic anomalies for varying inclination in a single dyke.

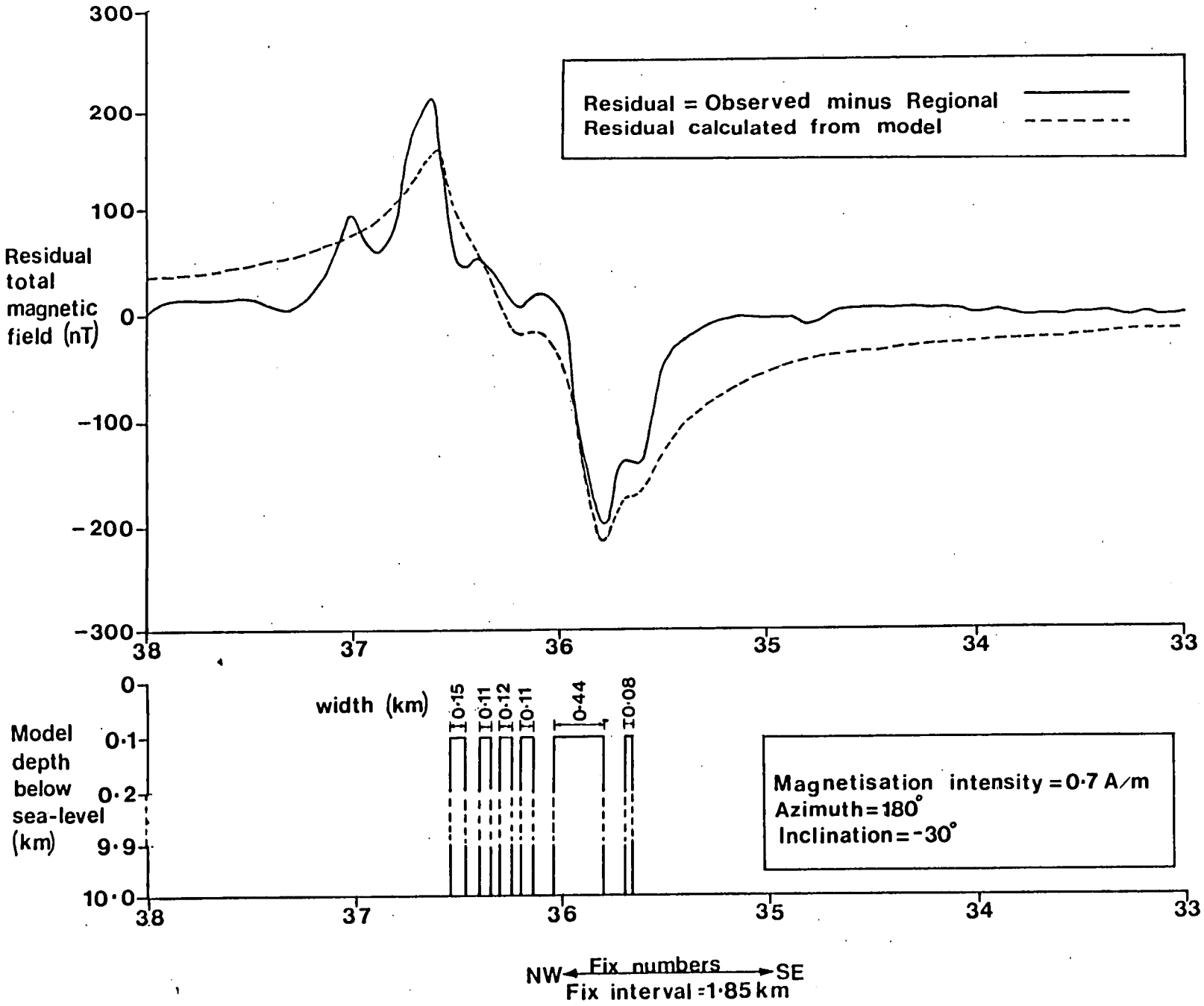

Fig 4.8 Calculated residual magnetic anomaly and dyke model, with 6 reversely magnetised dykes.

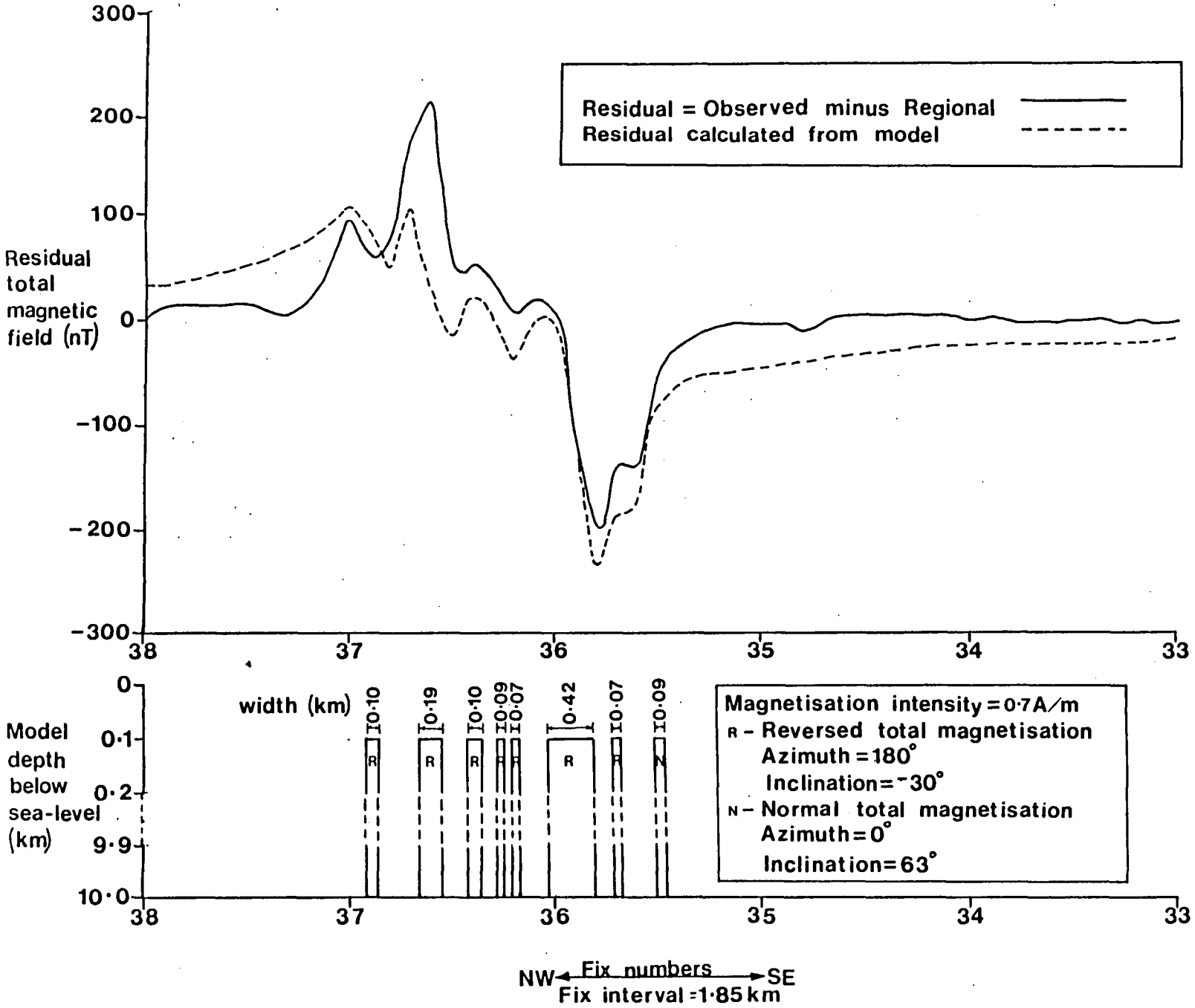

Fig 4.9 Calculated residual magnetic anomaly and dyke model, with 1 normally magnetised dyke and 7 reversely magnetised dykes.

References

Abraham, D. in prep. Bouguer anomaly map, Little Sole Bank, B.G.S. 1:250 000 series.

Abraham, D. in prep. Bouguer anomaly map, Cockburn Bank, B.G.S. 1:250 000 series.

Busby, J. P. 1986. Interactive 2.5D Gravity and Magnetic modelling on the ICL PERQ2. Rep. Reg. Geophys. Res. Group B.G.S. No RGRG 86/9.

Edwards, J.W.F. 1987. Aeromagnetic anomaly map, Little Sole Bank, B.G.S. 1:250 000 series.

Edwards, J.W.F., Briant, M. and Arthur, M. J. in prep. Geophysical evidence for a NE-SW Mesozoic dolerite dyke set, Haig Fras area, S. Celtic Sea.

Evans, C.D.R. (compiler). 1982. Solid geology map, Scilly. B.G.S. 1:250,000 series.

Evans, C.D.R. (compiler). 1985. Solid geology and seabed sediments maps, Parson's Bank B.G.S. 1:250,000 series.

Evans, C.D.R. (compiler). 1985. Solid geology map, Little Sole Bank, B.G.S. 1:250 000 series.

Evans, C.D.R. (compiler). 1985. Solid geology map, Cockburn Bank, B.G.S. 1:250 000 series.

Evans, C.D.R. and Hughes, M.J. 1984. The Neogene succession of the South Western Approaches, Great Britain. Journal of the Geological Society, 141, 315-326.

Evans, C.D.R., Lott, G.K. and Warrington, G. (compilers). 1981. The Zephyr (1977) wells, South Western Approaches and western English Channel. Report Institute of Geological Sciences, No 81/8.

Grant, F.S. and West, G.F. 1965. Interpretation theory in Applied Geophysics, McGraw-Hill P366.

Holder, M.T., Lott, G.K. and Bouysse, P.L. (compilers). 1983. Solid geology map, Lizard, B.G.S. 1:250,000 series.

Kirton, S.R. and Donato, J.A. 1985. Some buried Tertiary dykes of Britain and surrounding waters deduced by magnetic modelling and seismic reflection methods. Journal of the Geological Society, 142, 1047-57

Naylor, D. and Shannon, P. M. (eds) 1982. The Geology of Offshore Ireland and W Britain, Graham and Trotman, London.

Privé, E. 1987. Seismic Interpretation and gravity modelling of BIRPS SWAT lines 5 and 6. B.G.S. Marine report 87/14.

Smith, A. G., Hurley, A. M. and Briden, J. C. 1981. Phanerozoic palaeocontinential world maps. Cambridge University Press, Cambridge.

Smith, N. J. P. (compiler) 1985. Map 2: Contours on the top of the Pre-Permian surface of the United Kingdom (south), B.G.S.

Taylor, R. T., Bouysse, P. H., Fletcher, B. N. and Lefort, J. P. (compilers) 1980. Solid geology map, Gurnsey, B.G.S. 1:250 000 series.

Telford, W. M., Geldhart, L. P., Sheriff, R. E. and Keys, D. A. 1976. Applied Geophysics, Cambridge University Press.

Walker, J. R. 1981. Magrav: an interactive graphics computer, program for two-dimensional gravity/magnetics modelling. Marine Geophysical Computer Report, I.G.S. CP38.

Wilkinson, I.P. and Halliwell, G.P. (compilers). 1980. Offshore micropalaeontological biostratigraphy of southern and western Britain. Report Institute of Geological Sciences, No 79/9.